Published OnlineFirst July 6, 2011; DOI:10.1158/0008-5472.CAN-11-1076

Epigenetic gene silencing due to promoter CpG island (CGI) hypermethylation is one of the most common mechanisms by which TSGs are inactivated during tumorigenesis. In recent years, it has become evident that some miRNA genes are also targets of epigenetic silencing in cancer. Others and we have previously shown that pharmacologic or genetic disruption of DNA methylation in cancer cell lines induces upregulation of substantial numbers of miRNAs (5, 6). These analyses led to identification of candidate tumor-suppressive miRNAs whose silencing was associated with CGI methylation. For example, miR-127 is embedded in a typical CGI, and treatment of human bladder cancer cells with inhibitors of histone deacetylase (HDAC) and DNA methyltransferase (DNMT) induced CGI demethylation and reexpression of the miRNA (7). In addition, methylation of miR-124 family members (miR-124-1, -124-2, and -124-3) was identified in colorectal cancer and was subsequently reported in tumors of other origins (5). Similarly, we found frequent methylation and downregulation of miR-34b/c in both colorectal cancer and gastric cancer (6, 8).

Epigenetic regulation of miRNA genes is tightly linked to chromatin signatures. For instance, transcriptionally active miRNA genes are characterized by active chromatin marks, such as trimethylated histone H3 lysine 4 (H3K4me3; ref. 9). We previously showed that restoring H3K4me3 through DNA demethylation could be a useful marker for predicting the promoter region of a silenced miRNA gene (6). However, the chromatin signatures, including both active and repressive histone marks on miRNA genes, within the cancer genome are still largely unknown. In the present study, we carried out genome-wide profiling of chromatin signatures in colorectal cancer cells and identified the active promoter regions of miRNA genes. We also show that changes in chromatin signatures before and after the removal of DNA methylation lead to robust identification of miRNA genes that are epigenetically regulated in cancer.

Materials and Methods

Cell lines and tissue specimens

Colorectal cancer cell lines and HCT116 cells harboring genetic disruptions within the *DNMT1* and *DNMT3B* loci [double knockout (DKO)] have been described previously (6). Treatment of cells with 5-aza-2′-deoxycytidine (DAC; Sigma-Aldrich) and 4-phenylbutyrate (PBA; Sigma-Aldrich) was carried out as described (8). A total of 90 primary colorectal cancer specimens were obtained as described (6, 10). Samples of adjacent normal colorectal mucosa were also collected from 20 patients. A total of 78 colorectal adenoma specimens were obtained through endoscopic biopsy. Informed consent was obtained from all patients before collection of the specimens. Total RNA from normal colonic mucosa from healthy individuals was purchased from Ambion. Total RNA was extracted using a mirVana miRNA isolation kit (Ambion) or TRIzol reagent (Invitrogen). Genomic DNA was extracted using the standard phenol–chloroform procedure.

miRNA expression profiling

Expression of 470 miRNAs was analyzed using Human miRNA Microarray V1 (G4470A; Agilent Technologies) as described previously (8). In addition, expression of 664 miRNAs was analyzed using a TaqMan microRNA Array v2.0 (Applied Biosystems). Briefly, 1 μg of total RNA was reverse transcribed using Megaplex Pools kit (Applied Biosystems), after which the miRNAs were amplified and detected using PCR with specific primers and TaqMan probes. The PCR was run in a 7900HT Fast Real-Time PCR system (Applied Biosystems), and SDS2.2.2 software (Applied Biosystems) was used for comparative ΔC_t analysis. U6 snRNA (RNU6B; Applied Biosystems) served as an endogenous control. Microarray data and TaqMan Array data (ΔC_t values) were further analyzed using GeneSpring GX ver. 11 (Agilent Technologies). The Gene Expression Omnibus accession number for the microarray data is GSE29900.

Real-time reverse transcriptase PCR of miRNA

Expression of selected miRNAs was analyzed using TaqMan microRNA Assays (Applied Biosystems). Briefly, 5 ng of total RNA was reverse transcribed using specific stem-loop RT primers, after which the miRNAs were amplified and detected using PCR with specific primers and TaqMan probes as described earlier. U6 snRNA (RNU6B) served as an endogenous control. Expression of the primary miR-1-1 transcript was analyzed using a TaqMan Pri-miRNA assay (assay ID Hs03303345_pri; Applied Biosystems). Glyceraldehyde-3-phosphate dehydrogenase (GAPDH; assay ID Hs99999905_m1; Applied Biosystems) served as an endogenous control.

Chromatin immunoprecipitation-on-chip analysis

Chromatin immunoprecipitation (ChIP)-on-chip analysis was carried out according to Agilent Mammalian ChIP-on-chip Protocol version 10.0 (Agilent Technologies). Briefly, 1×10^8 cells were treated with 1% formaldehyde for 10 minutes to cross-link histones with the DNA. After washing with PBS, the cell pellets were resuspended in 3 mL of lysis buffer and sonicated. Chromatin was immunoprecipitated for 16 hours at 4°C using 10 μL of anti-trimethyl histone H3K4 (clone MC315; Upstate), anti-trimethyl histone (clone H3K27; Upstate) or anti-dimethyl histone H3K79 (clone NL59; Upstate) antibody. Before adding antibodies, 50 μL of the each cell lysate was saved as an internal control for the input DNA. After washing, elution, and reversal of the cross-links, input DNA and the immunoprecipitate were ligated to linkers and PCR amplified. Input DNA and the immunoprecipitate were then labeled with Cy3 and Cy5 using an Agilent Genomic DNA Enzymatic Labeling kit (Agilent Technologies) and hybridized to the 244K Human Promoter ChIP-on-chip microarray (G4489A; Agilent technologies). After washing, the array was scanned using an Agilent DNA Microarray scanner (Agilent Technologies), and the data were processed using Feature Extraction software (Agilent Technologies).

ChIP-seq analysis

ChIP experiments were carried out as described earlier, after which massively parallel sequencing was carried out

Published OnlineFirst July 6, 2011; DOI:10.1158/0008-5472.CAN-11-1076

using a SOLiD3 Plus system (Applied Biosystems) according to the manufacturer's instructions. Briefly, 100 ng of input DNA or the immunoprecipitate was ligated to adapters and PCR amplified using a SOLiD Fragment Library Construction kit (Applied Biosystems). Template bead preparation was carried out using a SOLiD ePCR kit V2 (Applied Biosystems) and a SOLiD Bead Enrichment kit (Applied Biosystems). Approximately 40 to 50 million beads per sample were sequenced using SOLiD Opti Fragment Library Sequencing Master Mix 50 (Applied Biosystems) and a SOLiD3 Plus sequencer (Applied Biosystems). Sequence reads that were of poor quality or those that were not uniquely mapped were excluded from the study. Peaks were identified using the Model-based Analysis for ChIP-seq (MACS) software (11) and visualized using the University of California Santa Cruz (UCSC) genome browser.

Reference sequence

Genomic locations are based on the UCSC hg18 (National Center for Biotechnology Information Build 36.1, March 2006), which was produced by the International Human Genome Sequencing Consortium. We also obtained locations of CGIs, ReSeq genes, and UCSC genes from the UCSC hg18 data sets.

Methylation analysis

Genomic DNA (2 μg) was modified with sodium bisulfite using an EpiTect Bisulfite kit (QIAGEN). Methylation-specific PCR (MSP), bisulfite sequencing, and bisulfite pyrosequencing were carried out as described (6). For bisulfite sequencing analysis, amplified PCR products were cloned into pCR2.1-TOPO vector (Invitrogen), and 10 to 12 clones from each sample were sequenced using an ABI3130x automated sequencer (Applied Biosystems). Primer sequences and PCR product sizes are listed in Supplementary Table S1.

Transfection of miRNA precursor molecules

Colorectal cancer cells (1×10^6 cells) were transfected with 100 pmol of Pre-miR miRNA Precursor Molecules (Ambion) or Pre-miR miRNA Molecules Negative Control #1 (Ambion) using a Cell Line Nucleofector kit V (Lonza) with a Nucleofector I electroporation device (Lonza) according to the manufacturer's instructions. Total RNA or cell lysate was extracted 48 hours after transfection. Cell viability assays, Western blotting, wound-healing assays, and Matrigel invasion assays are described in the Supplementary Methods.

Gene expression profiling

Total RNA (700 ng) was amplified and labeled using a Quick Amp Labeling kit one-color (Agilent Technologies), after which the synthesized cRNA was hybridized to the Whole Human Genome Oligo DNA microarray (G4112F; Agilent technologies). Data analysis was carried out using GeneSpring GX ver. 11 (Agilent technologies). The Gene Expression Omnibus accession number for the microarray data is GSE29760.

miRNA target predictions and luciferase reporter assays

The predicted targets of miR-1 and their downstream target sites were analyzed using TargetScan and miRanda. Construction of luciferase reporter vectors containing the predicted target sites and dual luciferase reporter assays were carried out as described in Supplementary Methods.

Results

miRNA profiling in colorectal cancer cell lines

To screen for epigenetically silenced miRNAs, we first carried out miRNA microarray analysis in a series of colorectal cancer cell lines (HCT116, DLD1, and RKO) and normal colonic tissue. Hierarchical clustering analysis revealed that expression of a majority of miRNAs was downregulated in all 3 colorectal cancer cell lines tested, as compared with normal colonic mucosa (Supplementary Fig. S1A). DAC treatment upregulated expression of a large number of miRNAs in all 3 colorectal cancer cell lines (Supplementary Fig. S1B), and combination treatment with DAC plus PBA induced even greater numbers of miRNAs in colorectal cancer cells (Supplementary Fig. S1C and D). However, the most profound effect on the miRNA expression profile was induced by genetic disruption of *DNMT1* and *DNMT3B* in HCT116 cells (DKO cells; Supplementary Fig. S1C). We also noted a novel overlap between miRNAs upregulated by pharmacologic or genetic disruption of DNA methylation and those downregulated in colorectal cancer cells, as compared with normal colonic mucosa (Supplementary Fig. S1E–G). To test the tumor-suppressive potentials of the downregulated miRNAs, we constructed expression vectors encoding selected miRNAs and carried out colony formation assays. We found that a majority of miRNAs exerted growth-suppressive effects when they were ectopically expressed in colorectal cancer cells (Supplementary Fig. S2). These results suggest that an epigenetic mechanism plays an essential role in the downregulation of a number of miRNAs in cancer and that such downregulation of numerous miRNAs may contribute to tumorigenesis.

Chromatin signatures of active and silenced miRNA genes

We next examined the chromatin signatures of miRNA genes in HCT116 colorectal cancer cells, with and without genetic disruption of *DNMT1* and *DNMT3B* (DKO cells). We carried out ChIP analysis using antibodies against trimethylated histone H3 lysine 4 (H3K4me3), which marks active promoters; dimethylated histone H3 lysine 79 (H3K79me2), which is associated with transcriptional elongation; and trimethylated histone H3 lysine 27 (H3K27me3), which is a repressive mark. We started our analysis using the Agilent 244K Promoter Array, which covers approximately 370 human miRNA genes, and we subsequently migrated to ChIP-seq analysis to increase our scope within the genome. We observed a good correlation between the results of the ChIP-on-chip and ChIP-seq analyses (Supplementary Fig. S3). We also validated the reliability of our ChIP-seq data by checking representative protein-coding genes that were transcriptionally active or silenced in HCT116 cells (Supplementary Fig. S4).

Representative chromatin signatures of miRNA genes are shown in Fig. 1A. We found enrichment of the H3K4me3 mark around the proximal upstream CGI regions of 2 abundantly

Published OnlineFirst July 6, 2011; DOI:10.1158/0008-5472.CAN-11-1076

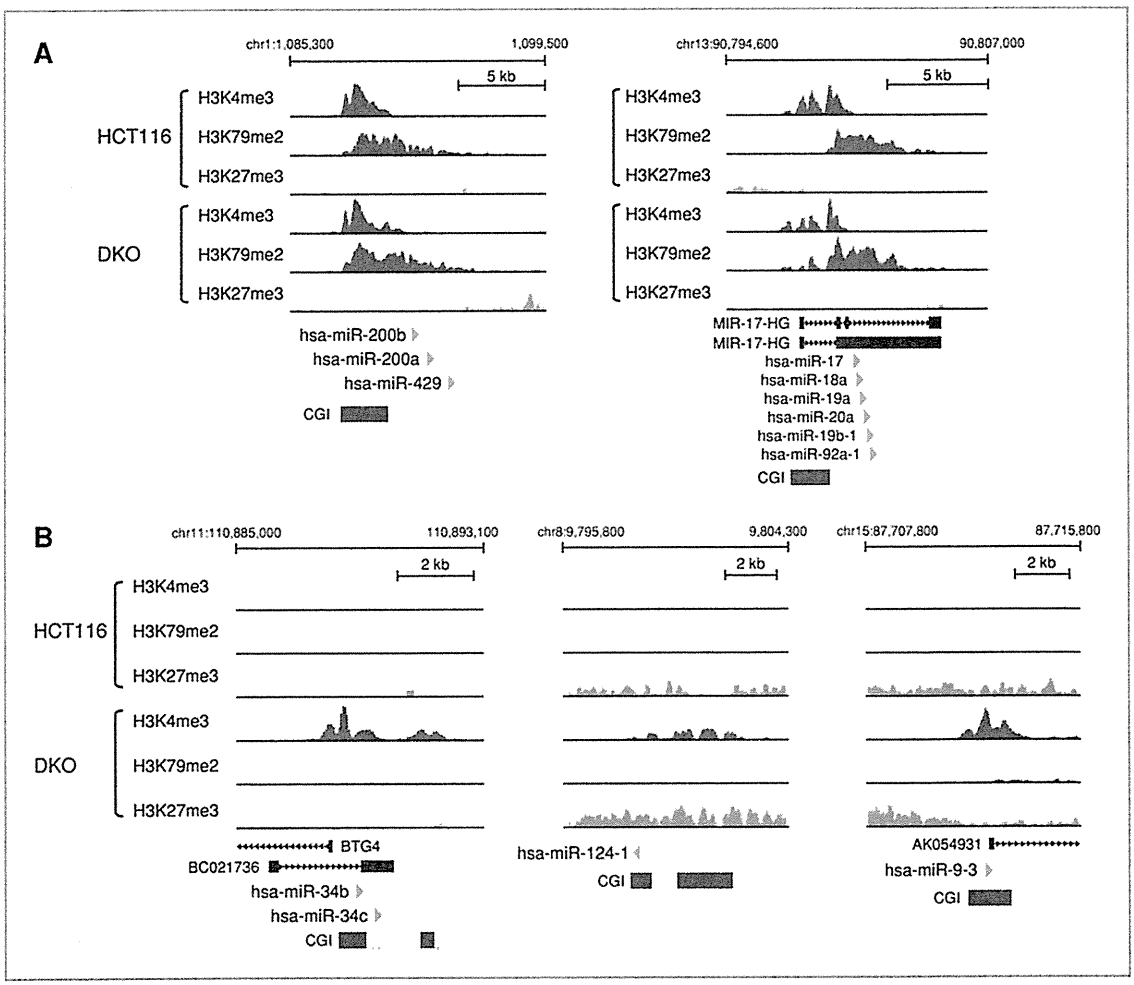

Figure 1. Chromatin signatures of transcriptionally active and epigenetically silenced miRNA genes in colorectal cancer. A, ChIP-seq results for H3K4me3, H3K79me2, and H3K27me3 in transcriptionally active miRNA genes in HCT116 and DKO cells. Chromosomal locations are indicated on the top. Locations of host genes, pre-miRNA genes, and CGIs are shown below. B, ChIP-seq results for epigenetically silenced miRNAs with associated CGI hypermethylation. CGI methylation is lost and miRNAs are reexpressed in DKO cells. H3K4me3 marking is upregulated in the putative promoter regions in DKO cells, whereas H3K79me2 shows only a minimal increase.

expressed miRNA clusters, miR-200b and miR-17, in both wild-type HCT116 and DKO cells (Fig. 1A). Gene bodies were marked by H3K79me2, which indicates active transcriptional elongation, whereas they almost completely lacked the repressive H3K27me3 mark. With respect to the H3K4me3 mark in the miR-17 cluster, we observed a sharp dip at the transcription start site (TSS) of the host gene and another dip downstream, which is consistent with a previous report that miR-17 has its own TSS within the intron of the host gene (Fig. 1A; ref. 12).

In contrast, miRNAs whose silencing was associated with promoter CGI hypermethylation completely lacked both of the active histone marks. The CGIs of miR-34b/c, miR-124-1, and miR-9-3 were densely methylated in HCT116 cells (5, 6, 13) and were completely devoid of H3K4me3 and H3K79me2 marks (Fig. 1B). miR-124-1 and miR-9-3 showed moderate enrichment of H3K27me3, whereas miR-34b/c was almost H3K27me3 free, which corresponds to previous reports that DNA methylation and H3K27me3 are sometimes observed independently in cancer (14). In DKO cells, where DNA methylation was significantly diminished and gene expression was restored, increased H3K4me3 marks were found at the upstream CGI, though restoration of H3K79me2 was quite limited. Upregulation of H3K27me3 was also seen around miR-124-1 and miR-9-3, which is consistent with previous observations that genes with methylated CGIs adopt a bivalent chromatin pattern after DNA demethylation (15, 16).

Published OnlineFirst July 6, 2011; DOI:10.1158/0008-5472.CAN-11-1076

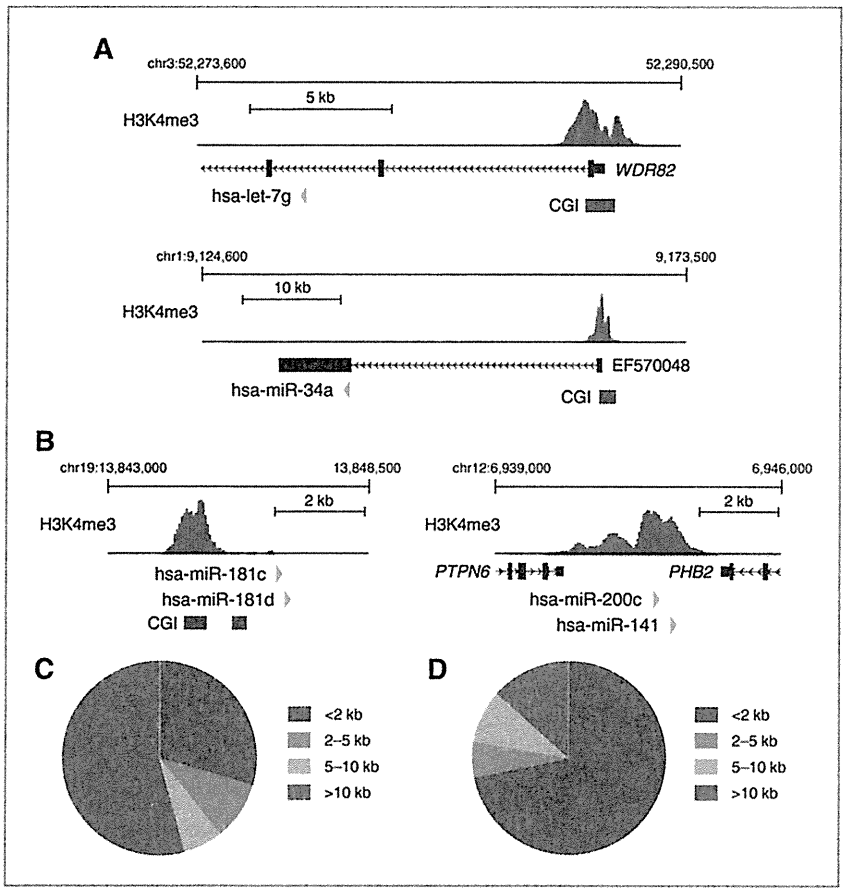

Figure 2. Identification of miRNA gene promoter regions using chromatin signatures. A, examples of H3K4me3 marks in intragenic miRNAs. Let-7g is located within the intron of the protein-coding gene *WDR82*, and miR-34a is located within the exon of a noncoding host gene. H3K4me3 marks are observed in the TSS regions of the host genes, suggesting that these miRNAs share common promoters with their host genes. B, examples of H3K4me3 marking of intergenic miRNA genes. C, summarized distances between intragenic pre-miRNA coding regions and their putative promoter regions ($n = 166$). D, summarized distances between intergenic pre-miRNA coding regions and their putative promoter regions ($n = 67$).

Identification of putative miRNA promoter regions

Identification of epigenetically silenced miRNAs is sometimes hampered by a lack of knowledge of the transcription initiation region of the primary miRNA transcripts. Previous studies have shown that H3K4me3 is a useful marker for identifying active miRNA gene promoters (9, 12), and we employed that approach with colorectal cancer cells. Using miRNA microarrays and TaqMan low-density arrays, we detected expression of 339 and 429 distinct mature miRNAs in HCT116 and DKO cells, respectively. We then searched for the putative promoter regions of these miRNAs, using H3K4me3 as a marker.

More than half of miRNAs are located in the introns of protein-coding or long noncoding RNA genes, and it is generally believed that intragenic miRNAs share common promoters with their host genes (17). We identified the putative promoters of 166 intragenic miRNAs located in RefSeq genes and/or UCSC genes, and a majority of the H3K4me3 marks were observed at the TSS of the host genes, many of which were located more than 10 kb upstream of the pre-miRNA coding regions (Fig. 2A and C, Supplementary Fig. S5A, and Supplementary Table S2). In contrast, intragenic H3K4me3 marks were identified in the proximal upstream of 22 pre-miRNAs, indicating these miRNAs have their own promoters and are transcribed independently of their host genes (Supplementary Fig. S6, Supplementary Table S3). To identify promoters of intergenic miRNAs, we first searched 10 kb upstream for H3K4me3 marks and also explored the initiation sites of overlapping 5′ expressed sequence tags (EST). We identified the putative promoters of 66 intergenic miRNAs, the majority of which (47 of 66) were identified in the proximal upstream (<2 kb) of the pre-miRNA coding region (Fig. 2B and D, Supplementary Fig. S5B, and Supplementary Table S2). In total, we identified the putative promoters of 174 transcript units encoding 233 distinct pre-miRNAs, whereas promoters of 135 miRNAs remain unidentified, despite their positive expression in colorectal cancer cells.

We validated our promoter search by comparing our results with previously reported transcription initiation regions. Promoters of 177 pre-miRNAs that we identified overlapped with those identified in human embryonic stem (ES) cells by Marson and colleagues (9), whereas only the promoters of 38 pre-miRNAs did not match. Similarly, the TSS of 65 miRNAs identified in human melanoma and breast cancer cell lines by

Published OnlineFirst July 6, 2011; DOI:10.1158/0008-5472.CAN-11-1076

Ozsolak and colleagues overlapped with the promoters we identified (12). For example, we found H3K4me3 marks overlapping with known TSS of the miR-17 cluster, let-7a-1/let-7f-1/let-7d, and miR-200c/141 (Fig. 2B, Supplementary Fig. S5). We also identified an H3K4me3 mark at the intronic transcription initiating region of miR-21 (Supplementary Fig. S6C). The high degree of consistency between our results and those of earlier studies attests to the accuracy of our promoter prediction.

Identification of epigenetically silenced miRNAs

We next endeavored to identify epigenetically silenced miRNA genes by taking advantage of the observation that DNA demethylation can induce increases in H3K4me3 in the promoters of the epigenetically silenced genes (6). We searched for miRNA genes showing reduction or loss of both expression and H3K4me3 marks in HCT116 and DKO cells. We identified 47 pre-miRNA genes encoded in 37 primary transcription units as potential targets of epigenetic silencing in HCT116 cells. Promoters of 22 transcription units were associated with CGIs, and MSP analysis revealed that all of the CGIs were methylated (Fig. 3A and B, Table 1). In most cases, DNA demethylation led to increases in H3K4me3 and H3K27me3 marking of the methylated CGIs of miRNA genes, whereas H3K79me2 marks were not restored by demethylation (Fig. 3C). In contrast, the chromatin signatures of miRNAs without promoter CGIs were more variable among genes. We

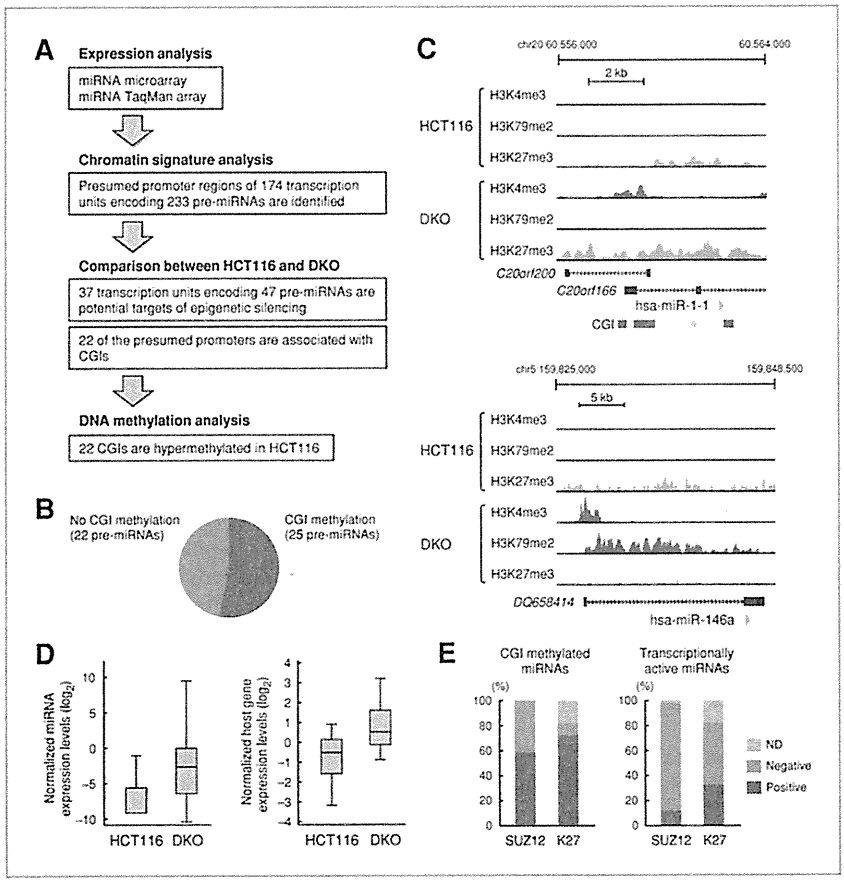

Figure 3. Identification of epigenetically silenced miRNA genes. A, flowchart for the selection of epigenetically silenced miRNA genes in colorectal cancer. B, graph showing the number of epigenetically silenced miRNAs associated with CGI methylation and those without CGI methylation. C, chromatin signatures of 2 representative miRNA genes, with and without promoter CGI methylation. miR-1-1 (top) was silenced in association with CGI methylation in HCT116 cells. In DKO cells, H3K4me3 marking was observed around the transcription start site of the host gene *C20orf166*. miR-146a (bottom) is another candidate target for epigenetic silencing in HCT116, though its promoter is not associated with CGI. Both H4K4me3 and H3K79me2 were restored in DKO cells. D, expression levels of epigenetically silenced miRNAs and their host genes in HCT116 and DKO cells. TaqMan real-time PCR data for 57 mature miRNAs encoded by 47 pre-miRNA genes were imported into Gene Spring GX, after which the data were normalized and shown in box plots (left). Expression data of 13 host genes of epigenetically silenced miRNAs were obtained using an Agilent Whole Human Genome microarray (right). E, miRNAs targeted by the PcG group in ES cells are more likely to be silenced by CGI hypermethylation in colorectal cancer cells. CGI-methylated miRNAs ($n = 22$; left) or transcriptionally active miRNAs ($n = 146$; right) were selected, and their SUZ12 binding and H3K27me3 enrichment in human ES cells were assessed. Of 22 CGI-methylated miRNAs, 13 (59%) were positive for SUZ12 and 16 (73%) for H3K27me3. ND, not determined.

Published OnlineFirst July 6, 2011; DOI:10.1158/0008-5472.CAN-11-1076

Table 1. Epigenetically silenced miRNA genes in HCT116

Name	miRNA position	Strand	Gene/EST	DKO H3K4me3	Distance	CpG	Methylation
hsa-mir-137	chr1:98284213-98284315	–	*AK311400*	chr1:98282607-98285011	<2 kb	CGI	M
hsa-mir-488	chr1:175265121-175265204	–	*ASTN1*	chr1:175267182-175269163	<2 kb	–	
hsa-mir-205	chr1:207672100-207672210	+	*LOC642587*	chr1:207668045-207668780	2–5 kb	–	
hsa-mir-10b	chr2:176723276-176723386		EST: BQ722165	chr2:176720798-176721389	<2 kb	CGI	M
hsa-mir-885	chr3:10411172-10411246	–	*ATP2B2*	chr3:10723790-10724643	>10 kb	–	
hsa-mir-944	chr3:191030404-191030492	+	*TP63*	chr3:190831254-190831806	>10 kb	–	
hsa-mir-146a	chr5:159844936-159845035	+	*DQ658414*	chr5:159827186-159829843	>10 kb	–	
hsa-mir-218-2	chr5:168127728-168127838	–	*SLIT3*	chr5:168127234-168128479	<2 kb	–	
hsa-mir-9-2	chr5:87998426-87998513	–	*LOC645323*	chr5:87997315-87999774	<2 kb	–	
hsa-mir-548b	chr6:119431910-119432007	–	*FAM184A*	chr6:119440287-119442581	5–10 kb	CGI	M
hsa-mir-129-1	chr7:127635160-127635232	+		chr7:127628134-127629349	5–10 kb	CGI	M
hsa-mir-153-2	chr7:157059788-157059875	–	*PTPRN2*	chr7:157061089-157064064	<2 kb	CGI	M
hsa-mir-596	chr8:1752803-1752880	+		chr8:1751984-1754090	<2 kb	CGI	M
hsa-mir-124-1	chr8:9798307-9798392	–		chr8:9798198-9799439	<2 kb	CGI	M
hsa-mir-598	chr8:10930125-10930222	–	*XKR6*	chr8:11094125-11097386	>10 kb	CGI	M
hsa-mir-486	chr8:41637115-41637183	–	*ANK1*	chr8:41660039-41661630	>10 kb	–	
hsa-mir-124-2	chr8:65454259-65454368	+	*BX537900*	chr8:65452660-65453362	<2 kb	CGI	M
hsa-mir-876	chr9:28853623-28853704	–	EST: DA506041	chr9:29200954-29205760	>10 kb	CGI	M
hsa-mir-873	chr9:28878876-28878953	–	EST: DA506041	chr9:29200954-29205760	>10 kb	CGI	M
hsa-mir-146b	chr10:104186258-104186331	+		chr10:104185067-104186052	<2 kb	–	
hsa-mir-129-2	chr11:43559519-43559609	+	EST: BI964058	chr11:43556836-43561086	<2 kb	CGI	M
hsa-mir-708	chr11:78790713-78790801	–	*ODZ4*	chr11:78825491-78830366	>10 kb	CGI	M
hsa-mir-34b	chr11:110888872-110888956	+	*BC021736*	chr11:110887701-110889527	<2 kb	CGI	M
hsa-mir-34c	chr11:110889373-110889450	+	*BC021736*	chr11:110887701-110889527	<2 kb	CGI	M
hsa-mir-337	chr14:100410582-100410675	+		chr14:100407328-100408197	2–5 kb	–	
hsa-mir-431	chr14:100417096-100417210	+		chr14:100417110-100420818	<2 kb	–	
hsa-mir-433	chr14:100417975-100418068	+		chr14:100417110-100420818	<2 kb	–	
hsa-mir-127	chr14:100419068-100419165	+		chr14:100417110-100420818	<2 kb	CGI	M
hsa-mir-432	chr14:100420572-100420666	+		chr14:100417110-100420818	<2 kb	–	
hsa-mir-136	chr14:100420791-100420873	+		chr14:100417110-100420818	<2 kb	–	
hsa-mir-211	chr15:29144526-29144636	–	*TRPM1*	chr15:29160209-29160816	>10 kb	–	
hsa-mir-190	chr15:60903208-60903293	+	*TLN2*	chr15:60769608-60770528	>10 kb	–	
hsa-mir-9-3	chr15:87712251-87712341	+	*CR612213*	chr15:87711049-87714084	<2 kb	CGI	M
hsa-mir-195	chr17:6861657-6861744	–	EST: DA285925	chr17:6862382-6864312	<2 kb	–	
hsa-mir-497	chr17:6861953-6862065	–	EST: DA285925	chr17:6862382-6864312	<2 kb	–	
hsa-mir-193a	chr17:26911127-26911215	+		chr17:26910360-26912430	<2 kb	CGI	M
hsa-mir-152	chr17:43469525-43469612	–	*COPZ2*	chr17:43468887-43470981	<2 kb	CGI	M
hsa-mir-196a-1	chr17:44064850-44064920	–	EST:AI222881	chr17:44065082-44066831	<2 kb	CGI	M
hsa-mir-142	chr17:53763591-53763678	–	*AK311311* (antisense)	chr17:53762545-53765705	<2 kb	–	
hsa-mir-338	chr17:76714277-76714344	–	*AATK*	chr17:76753247-76754663	>10 kb	CGI	M
hsa-mir-371	chr19:58982740-58982807	+		chr19:58982297-58983364	<2 kb	–	
hsa-mir-372	chr19:58982955-58983022	+		chr19:58982297-58983364	<2 kb	–	
hsa-mir-373	chr19:58983770-58983839	+		chr19:58982297-58983364	<2 kb	–	
hsa-mir-1-1	chr20:60561957-60562028	+	*C20orf166*	chr20:60557701-60559681	2–5 kb	CGI	M
hsa-mir-133a-2	chr20:60572563-60572665	+	*C20orf166*	chr20:60557701-60559681	>10 kb	CGI	M
hsa-mir-124-3	chr20:61280296-61280383	+		chr20:61276185-61277804	2–5 kb	CGI	M
hsa-mir-155	chr21:25868162-25868227	+	*MIR155HG*	chr21:25855844-25857551	>10 kb	CGI	M

Abbreviations: gene/EST, overlapping gene or EST; distance, distance between pre-miRNA coding region and presumed promoter; CGI, CpG island positive at the promoter; M, CGI methylated.

Published OnlineFirst July 6, 2011; DOI:10.1158/0008-5472.CAN-11-1076

noted that a small number of non-CGI miRNAs acquired more active chromatin states upon DNA demethylation than did CGI-methylated miRNAs. For instance, miR-146a is characterized by a lack of active histone marks and enrichment of H3K27me3, but it showed restoration of both H3K4me3 and H3K79me2 in DKO cells (Fig. 3C). We observed similar upregulation of both active marks in miR-142 (Supplementary Fig. S7E). Weak basal expression of these miRNAs, detectable by TaqMan assay but not by microarray, and robust upregulation after DNA demethylation indicate that the silencing of these miRNAs is less stringent than that of miRNAs with methylated CGIs (data not shown).

DNA demethylation significantly upregulated the expression of mature miRNAs derived from 47 silenced pre-miRNAs (Fig. 3D). In addition, expression data from 13 host genes of the silenced miRNAs were obtained from Agilent gene expression microarray analysis (6), and we observed a strong tendency for the host genes to be upregulated by DNA demethylation (Fig. 3E). Recent studies have shown that genes marked by polycomb (PcG) group proteins in ES cells have a predisposition toward DNA hypermethylation in cancer (18, 19). By comparison with previously published results (9), we found that miRNAs with SUZ12 binding and H3K27me3 marks in human ES cells are significantly enriched in CGI-methylated miRNAs in colorectal cancer (Fig. 3E).

We further analyzed CGI methylation in a series of colorectal cancer cell lines using MSP and bisulfite pyrosequencing and found that they are methylated to varying degrees (Fig. 4A, Supplementary Fig. S8). We also confirmed inverse relationships between methylation and expression of selected miRNAs in colorectal cancer cell lines and normal colonic tissue (Fig. 4B). To determine the extent to which these miRNA genes are aberrantly methylated in primary tumors, we carried out bisulfite pyrosequencing of 18 miRNA promoter CGIs in primary colorectal cancer tumors ($n = 90$) and normal colonic tissue obtained from colorectal cancer patients ($n = 20$; Supplementary Fig. S9). Most of the miRNA genes were methylated in a tumor-specific or tumor-predominant manner. The two exceptions were miR-153-2 and miR-196a-1, which were methylated to similar degrees in both normal colon and tumor tissues, as well as in various normal human tissues (Supplementary Figs. S9 and S10). Elevated levels of miRNA gene methylation (>15.0%) were frequently detected in primary colorectal cancer tumors (miR-1-1, 77.8%; miR-9-1, 57.8%; miR-9-3, 89.9%; miR-34b/c, 89.7%; miR-124-1, 87.7%; miR-124-2, 96.6%; miR-124-3, 100.0%; miR-128-2, 73.6%; miR-129-2, 40.0%; miR-137, 100.0%; miR-193a, 28.7%; miR-338, 15.6%; and miR-548b, 47.8%), whereas a small number of genes were rarely methylated in primary tumors (miR-152, 4.4%; miR-155, 6.7%; and miR-596, 2.3%).

MiR-1-1 is a candidate tumor suppressor gene in colorectal cancer

Among the epigenetically silenced miRNAs, we next focused on miR-1-1 because it has received relatively little attention in colorectal cancer despite its frequent hypermethylation in that disease. Using bisulfite pyrosequencing, we detected elevated levels (>15.0%) of miR-1-1 methylation in both primary colorectal cancer tumors and colorectal adenomas (54 of 78, 69.2%), suggesting that its methylation is an early event in colorectal tumorigenesis (Fig. 5A). In contrast, levels of miR-1-1 methylation were relatively low (<15.0%) in the normal colonic tissues tested (Fig. 5A). We carried out bisulfite sequencing analysis to confirm the methylation results in selected tissue specimens and colorectal cancer cell lines (Fig. 5B, Supplementary Fig. S11A and B). We also confirmed that DNA demethylation could restore expression of the primary transcript of miR-1-1 (pri-miR-1-1) in colorectal cancer cells (Supplementary Fig. S11C).

To determine whether miR-1-1 serves as a tumor suppressor in colorectal cancer, we transfected colorectal cancer cell lines with a miR-1 precursor molecule or a negative control and then carried out a series of MTT assays. Forty-eight hours after transfection, we observed that ectopic expression of miR-1 moderately suppressed growth in all 3 cell lines (Fig. 5C). Colony formation assays also revealed reduced colony formation by colorectal cancer cells transfected with a miR-1-1 expression vector (Fig. 5D).

To further clarify the effect of the miRNA, we next carried out a gene expression microarray analysis of HCT116 cells transfected with a miR-1 precursor molecule or a negative control. We found that 2,769 probe sets were downregulated (>1.5-fold) by ectopic miR-1 expression, and gene ontology analysis revealed that "extracellular regions," "membrane," and "response to wounding" genes were significantly enriched among the downregulated genes (Supplementary Table S4). The genes downregulated by miR-1 included a number of predicted miR-1 targets (Supplementary Table S5). Among them, we noted 2 genes, Annexin A2 (*ANXA2*) and brain-derived neurotrophic factor (*BDNF*), which have been implicated in tumor growth and metastasis (20–22). Reduction of their expression by miR-1 in colorectal cancer cells was confirmed by Western blotting and real-time reverse transcriptase PCR (RT-PCR; Fig. 5E, Supplementary Fig. S12A). Reporter assays using luciferase vectors containing the putative miR-1 binding sites revealed that cotransfection of a miR-1 precursor molecule markedly reduced luciferase activities and that such reductions were not induced by a negative control or an irrelevant miRNA molecule (Fig. 5F and G, Supplementary Fig. S12B and S12C). Finally, we carried out wound-healing and Matrigel invasion assays to test the effect of miR-1 expression on colorectal cancer cell migration and invasion. We found that wound closure by HCT116 cells transfected with the negative control was complete within 28 hours whereas miR-1–expressing cells migrated toward the wound at a much slower rate (Fig. 5H). We also observed significant inhibition of cell invasion by miR-1 in HCT116 cells (Fig. 5I). These results strongly suggest that miR-1 acts as a tumor suppressor in colorectal cancer.

Discussion

In the present study, we provide a comprehensive view of the epigenetic regulation of miRNA genes in colorectal cancer cells. Because of the poor annotation of primary miRNA genes, the precise locations of the promoters and TSSs are not fully understood yet. To overcome these difficulties, earlier studies have searched for specific genomic features including RNA

Published OnlineFirst July 6, 2011; DOI:10.1158/0008-5472.CAN-11-1076

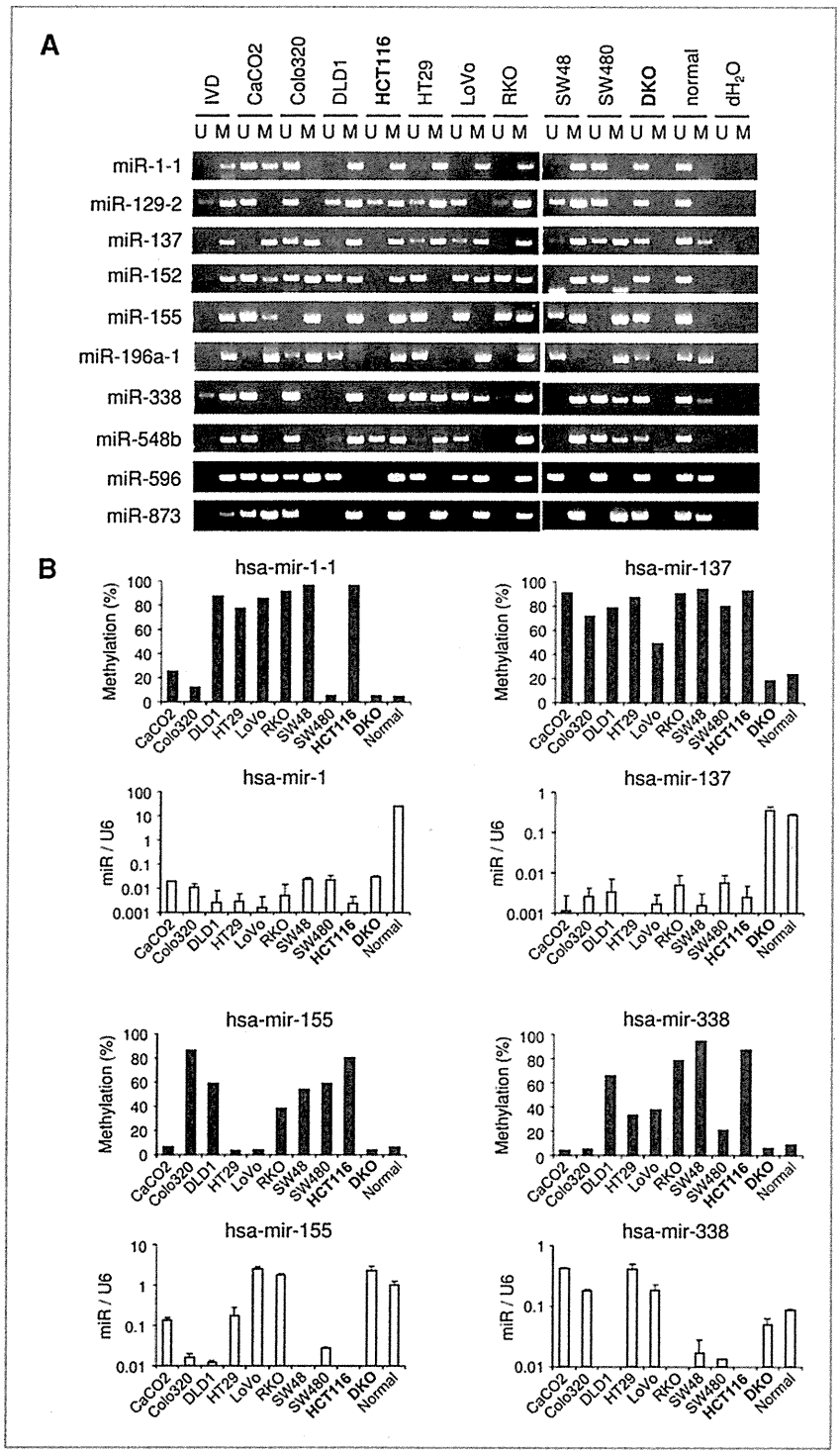

Figure 4. DNA methylation and expression analysis of miRNAs in colorectal cancer cells. A, representative results of MSP analysis of a series of colorectal cancer cell lines and normal colonic tissue. Bands in the "M" lanes are PCR products obtained with methylation-specific primers; those in the "U" lanes are products obtained with unmethylated-specific primers. *In vitro* methylated DNA (IVD) serves as a positive control. B, relationship between DNA methylation and expression of miRNAs in colorectal cancer. Bisulfite pyrosequencing results for miRNA promoter CGIs (black bars) and TaqMan real-time PCR results for mature miRNAs (gray bars) in a series of colorectal cancer cell lines and normal colonic tissue are shown. RT-PCR results were normalized to internal U6 snRNA expression.

Published OnlineFirst July 6, 2011; DOI:10.1158/0008-5472.CAN-11-1076

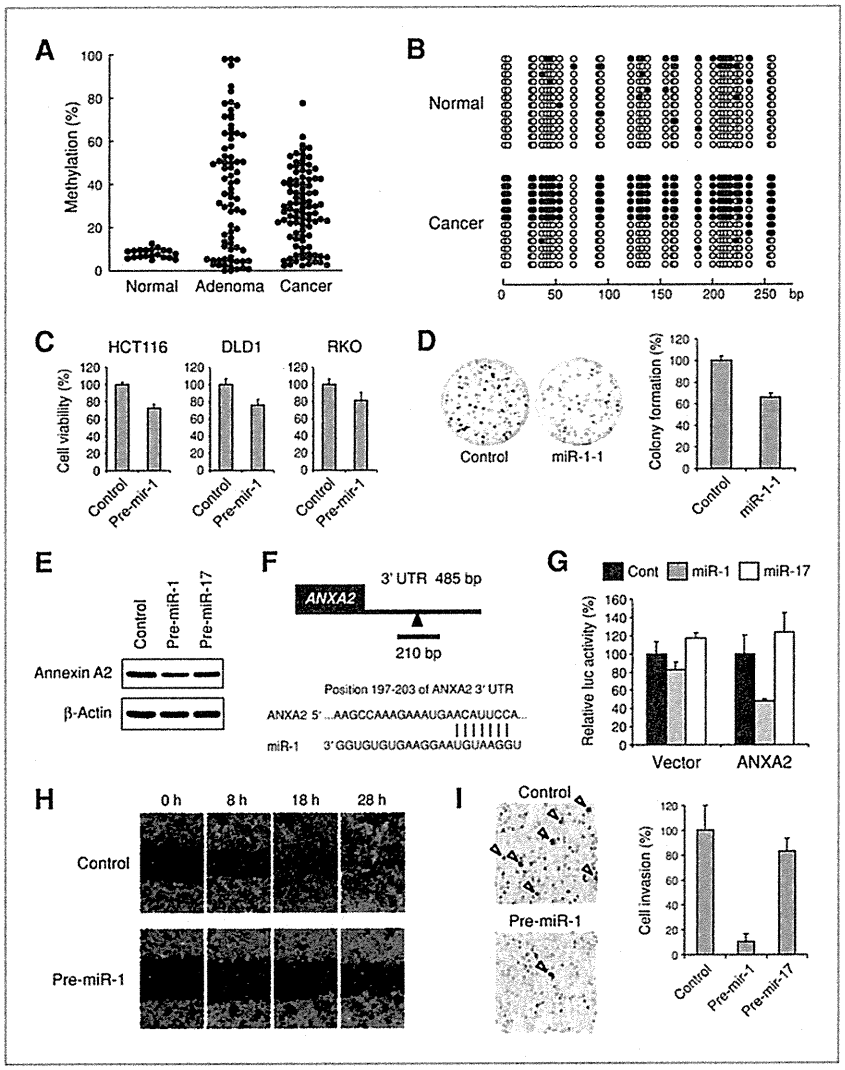

Figure 5. Methylation and functional analysis of miR-1-1 in colorectal cancer. A, summarized bisulfite pyrosequencing results for the miR-1-1 promoter CGI in normal colonic tissue ($n = 20$), colorectal adenomas ($n = 78$), and primary colorectal cancer tumors ($n = 90$). B, representative bisulfite sequencing results for the miR-1-1 promoter in a sample of normal colonic tissue and a primary colorectal cancer tumor. Open and filled circles represent unmethylated and methylated CpG sites, respectively. C, MTT assays with colorectal cancer cell lines transfected with a miR-1 precursor molecule or a negative control. Cell viabilities were determined 48 hours after transfection. Values were normalized to cells transfected with the negative control. Shown are the means of 8 replications; error bars represent SDs. D, colony formation assays using HCT116 cells transfected with a miR-1-1 expression vector or a control vector. Representative results are shown on the left, and relative colony formation efficiencies are on the right. Shown are means of 3 replications; error bars represent SDs. E, Western blot analysis of Annexin A2 in HCT116 cells transfected with a miR-1 precursor molecule or a negative control. Precursor of miR-17, which is abundantly expressed in HCT116 cells and is irrelevant to miR-1, served as another negative control. F, putative miR-1 binding site in the 3′ untranslated region (UTR) of *ANXA2*. A fragment that included the binding site was PCR amplified and cloned into pMIR-REPORT vector. G, reporter assay results using the luciferase vector with the 3′ UTR of *ANXA2* or an empty vector in HCT116 cells cotransfected with a miR-1 precursor, a negative control (Cont), or a miR-17 precursor. Shown are the means of 4 replications; error bars represent SDs. H, wound-healing assay using HCT116 cells transfected with a miR-1 precursor or a negative control. The wound was made 24 hours after transfection, and photographs were taken at the indicated time points. I, Matrigel invasion assay using HCT116 cells transfected with a miR-1 precursor, a negative control, or a miR-17 precursor. Invading cells are indicated by arrowheads. Shown on the right are the means of 3 random microscopic fields per membrane; error bars represent the SDs.

polymerase (pol) II binding patterns (23, 24), evolutionally conserved regions (25), EST mapping (26), and computationally predicted promoters (27, 28). Active promoters are reportedly marked by H3K4me3 (29), and recent studies that have applied such histone marks have successfully identified miRNA gene promoters or TSSs (9, 12). In the present study,

Published OnlineFirst July 6, 2011; DOI:10.1158/0008-5472.CAN-11-1076

we carried out high-resolution ChIP-seq analyses in an effort to detect the chromatin signatures of miRNA genes in colorectal cancer.

Although we were able to identify the putative promoters of a number of miRNAs, the present study has several limitations. First, our strategy to identify miRNA promoters can be applied only to transcriptionally active genes. Second, promoters of 135 miRNAs remain unidentified, although their expression was detected in colorectal cancer cells. The majority of such miRNAs (103 of 135) are located in the intergenic regions, and if we increase our search scope, we may identify putative promoter regions in the further upstream, although the accuracy may be decreased. For example, in DKO cells, we detected abundant expression of placenta-specific miRNAs transcribed from a miRNA cluster on chromosome 19 (C19MC), suggesting these miRNAs are epigenetically silenced in normal adult tissues. We found an H3K4me3 mark around a CGI located approximately 18 kb upstream of the cluster, suggesting that this region may be a putative promoter of C19MC (Supplementary Fig. S13), which is consistent with a recent report that hypermethylation of this CGI is associated with epigenetic silencing of C19MC in human cancer cell lines (30). However, other studies have shown that the Alu repetitive sequences within which C19MC is embedded exhibit RNA pol II or pol III promoter activities (31, 32), but we failed to detect obvious active histone marks in these Alu repeats. These results suggest that C19MC may have multiple promoter regions and point to a limitation of the strategy we employed in the current study.

Despite this limitation, chromatin signatures provided important clues to the identity of epigenetically silenced miRNAs in cancer. In HCT116 cells, for instance, the miR-9-1 promoter showed significant enrichment of active histone marks and mature miR-9 was abundantly expressed (data not shown). On the other hand, lack of H3K4me3 in the same cells and its restoration after DNA demethylation clearly suggest that miR-9-2 and miR-9-3 are epigenetically silenced in these cells, which is indicative of the utility of our strategy. We also noted that chromatin signatures of epileptically silenced miRNA genes exhibit patterns similar to those of protein-coding genes. Recent studies have shown that TSGs with CGI methylation retain repressive histone modifications (H3K9me3 and H3K27me3) even after demethylation (15). A genome-wide analysis of the chromatin signature using ChIP-on-chip in colorectal cancer cells revealed that hypermethylated genes adopt a bivalent chromatin pattern upon DNA demethylation (16). More recently, Jacinto and colleagues found that DNA demethylation never results in restoration of the H3K79me2 mark in TSGs with methylated CGIs, suggesting that such incomplete chromatin reactivation leads to relatively low levels of reexpression (33). In the present study, we found that miRNA genes with methylated CGIs never return to a full euchromatin status after DNA demethylation. In addition, we observed significant overlap between PcG marked miRNAs in ES cells and miRNAs with CGI methylation in cancer cells, suggesting a strong predisposition of these miRNAs toward aberrant DNA methylation in cancer.

Many of the epigenetically silenced miRNA genes we identified have been implicated in human malignancies. miR-124 family, miR-9 family, miR-34b/c, and miR-129-2 were identified by screening for epigenetically silenced miRNAs in colorectal cancer cell lines (5, 6, 13), and their methylation was subsequently found in various cancers (8, 34–36). Methylation-associated silencing of miR-137 was first reported in oral cancer (37), and a recent study revealed its frequent methylation in the early stages of colorectal tumorigenesis (38). The high frequency of CGI hypermethylation in these miRNAs in primary colorectal cancer is suggestive of their tumor suppressor function. It was also recently shown that the muscle-specific miRNAs miR-1 and miR-133a are downregulated in primary colorectal cancer tumors as compared with normal colonic tissues (39). Reduced expression of miR-1 is also found in lung cancer (40), and CGI methylation–mediated silencing of miR-1-1 has been reported in hepatocellular carcinoma (41). In addition, levels of miR-1 expression were diminished in the serum of non–small-cell lung cancer (NSCLC) patients who survived for only a short period, suggesting that it is predictive of prognosis in NSCLC patients (42). Ectopic expression of miR-1 in lung cancer, liver cancer, and rhabdomyosarcoma cells reportedly inhibits cellular growth through suppression of its target genes, which include *MET*, *FOXP1*, and *HDAC4* (40, 41, 43). In the present study, we found frequent methylation of the miR-1-1 promoter CGI in both colorectal adenoma and primary colorectal cancer tissues, suggesting that aberrant methylation of miR-1-1 is an early event in colorectal tumorigenesis. The strong tumor specificity of the methylation indicates that it could be a novel tumor marker for early detection of colorectal neoplasia. Because the tumor suppressor potential of miR-1 has not been tested in colorectal cancer, we conducted a number of functional analyses, and our findings indicate that ectopic expression of miR-1 in colorectal cancer cells suppresses cell growth, colony formation, cell motility, and invasion. In addition, our gene expression analysis revealed that miR-1 could induce global changes in gene expression in colorectal cancer cells, especially genes related to the extracellular region, cell membrane, and wound healing. We identified 2 novel miR-1 target genes, *ANXA2* and *BDNF*, which are frequently overexpressed in cancer and are implicated in invasion and metastasis (20–22). These results are suggestive of the tumor suppressor role of miR-1 and its potential therapeutic application in colorectal cancer.

On the other hand, we unexpectedly detected silencing of several miRNAs with known oncogenic properties. For example, miR-155 is a well-characterized oncogenic miRNA that is overexpressed in various human malignancies (44). Although we found miR-155 to be silenced with CGI methylation in HCT116 cells, its methylation was rarely observed in primary tumors, suggesting that epigenetic silencing of miR-155 may not be functionally important in colorectal cancer. Similarly, miR-196a-1 is reportedly overexpressed in several human malignancies, including esophageal adenocarcinoma and glioblastoma (45, 46). Methylation levels of miR-196a-1 in primary colorectal cancer tumors are lower than in normal colonic tissue, which is in agreement with its possible oncogenic properties in colorectal cancer.

Finally, our chromatin signature analysis revealed that a number of miRNAs without promoter CGIs are also potential

Published OnlineFirst July 6, 2011; DOI:10.1158/0008-5472.CAN-11-1076

targets of epigenetic silencing in colorectal cancer. These miRNAs were identified through restoration of both their expression and H3K4me3 marking after DNA demethylation, whereas the signatures of H3K79me2 and H3K27me3 varied among genes. This category may thus include miRNAs induced by secondary effects of DNA demethylation, such as upregulation of transcription factors. It is noteworthy, however, that some functionally important miRNAs showed chromatin signatures that were distinct from CGI-methylated miRNAs. Upon DNA demethylation, miR-142 and miR-146a exhibited more active chromatin states, which were characterized by enrichment of both H3K4me3 and H3K79me2 marks. Earlier studies implicated their tumor suppressor roles in cancers of various origins. For instance, miR-142 was found to be downregulated in murine and human lung cancer and its expression suppressed cancer cell growth (47). Loss of miR-146a was reported in hormone-refractory prostate cancer (48), and expression of miR-146a suppressed NF-κB activity and metastatic potential in breast and pancreatic cancer cells (49, 50). The abundant expression of miRNAs in normal colon and downregulation in multiple colorectal cancer cell lines indicates their tumor-suppressive properties in colorectal cancer (data not shown), though further study is need to define the functions of miRNAs in colorectal tumorigenesis.

With this study, we provide compelling evidence that both CGI-positive and -negative miRNAs are targets of epigenetic silencing in colorectal cancer. Our data suggest that DNA demethylation can alter the chromatin signatures of numerous miRNAs in cancer and that reexpression of these miRNAs has important relevance to the effects of epigenetic cancer therapy.

Disclosure of Potential Conflicts of Interest

No potential conflicts of interest were disclosed.

Acknowledgments

The authors thank Dr. William F. Goldman for editing the manuscript and M. Ashida for technical assistance.

Grant Support

This study was supported in part by Grants-in-Aid for Scientific Research on Priority Areas (M. Toyota and K. Imai), a Grant-in-Aid for the Third-term Comprehensive 10-year Strategy for Cancer Control (M. Toyota), a Grant-in-Aid for Cancer Research from the Ministry of Health, Labor, and Welfare, Japan (M. Toyota), the A3 foresight program from the Japan Society for Promotion of Science (H. Suzuki), and Grants-in-Aid for Scientific Research (A) from the Japan Society for Promotion of Science (K. Imai).

The costs of publication of this article were defrayed in part by the payment of page charges. This article must therefore be hereby marked *advertisement* in accordance with 18 U.S.C. Section 1734 solely to indicate this fact.

Received March 27, 2011; revised June 28, 2011; accepted June 30, 2011; published OnlineFirst July 6, 2011.

References

1. He L, Hannon GJ. MicroRNAs: small RNAs with a big role in gene regulation. Nat Rev Genet 2004;5:522–31.
2. Esquela-Kerscher A, Slack FJ. Oncomirs—microRNAs with a role in cancer. Nat Rev Cancer 2006;6:259–69.
3. Melo SA, Ropero S, Moutinho C, Aaltonen LA, Yamamoto H, Calin GA, et al. A TARBP2 mutation in human cancer impairs microRNA processing and DICER1 function. Nat Genet 2009;41:365–70.
4. Melo SA, Moutinho C, Ropero S, Calin GA, Rossi S, Spizzo R, et al. A genetic defect in exportin-5 traps precursor microRNAs in the nucleus of cancer cells. Cancer Cell 2010;18:303–15.
5. Lujambio A, Ropero S, Ballestar E, Fraga MF, Cerrato C, Setien F, et al. Genetic unmasking of an epigenetically silenced microRNA in human cancer cells. Cancer Res 2007;67:1424–9.
6. Toyota M, Suzuki H, Sasaki Y, Maruyama R, Imai K, Shinomura Y, et al. Epigenetic silencing of microRNA-34b/c and B-cell translocation gene 4 is associated with CpG island methylation in colorectal cancer. Cancer Res 2008;68:4123–32.
7. Saito Y, Liang G, Egger G, Friedman JM, Chuang JC, Coetzee GA, et al. Specific activation of microRNA-127 with downregulation of the proto-oncogene BCL6 by chromatin-modifying drugs in human cancer cells. Cancer Cell 2006;9:435–43.
8. Suzuki H, Yamamoto E, Nojima M, Kai M, Yamano HO, Yoshikawa K, et al. Methylation-associated silencing of microRNA-34b/c in gastric cancer and its involvement in an epigenetic field defect. Carcinogenesis 2010;31:2066–73.
9. Marson A, Levine SS, Cole MF, Frampton GM, Brambrink T, Johnstone S, et al. Connecting microRNA genes to the core transcriptional regulatory circuitry of embryonic stem cells. Cell 2008;134:521–33.
10. Akino K, Toyota M, Suzuki H, Mita H, Sasaki Y, Ohe-Toyota M, et al. The Ras effector RASSF2 is a novel tumor-suppressor gene in human colorectal cancer. Gastroenterology 2005;129:156–69.
11. Zhang Y, Liu T, Meyer CA, Eeckhoute J, Johnson DS, Bernstein BE, et al. Model-based analysis of ChIP-Seq (MACS). Genome Biol 2008;9:R137.
12. Ozsolak F, Poling LL, Wang Z, Liu H, Liu XS, Roeder RG, et al. Chromatin structure analyses identify miRNA promoters. Genes Dev 2008;22:3172–83.
13. Bandres E, Agirre X, Bitarte N, Ramirez N, Zarate R, Roman-Gomez J, et al. Epigenetic regulation of microRNA expression in colorectal cancer. Int J Cancer 2009;125:2737–43.
14. Kondo Y, Shen L, Cheng AS, Ahmed S, Boumber Y, Charo C, et al. Gene silencing in cancer by histone H3 lysine 27 trimethylation independent of promoter DNA methylation. Nat Genet 2008;40:741–50.
15. McGarvey KM, Fahrner JA, Greene E, Martens J, Jenuwein T, Baylin SB. Silenced tumor suppressor genes reactivated by DNA demethylation do not return to a fully euchromatic chromatin state. Cancer Res 2006;66:3541–9.
16. McGarvey KM, Van Neste L, Cope L, Ohm JE, Herman JG, Van Criekinge W, et al. Defining a chromatin pattern that characterizes DNA-hypermethylated genes in colon cancer cells. Cancer Res 2008;68:5753–9.
17. Rodriguez A, Griffiths-Jones S, Ashurst JL, Bradley A. Identification of mammalian microRNA host genes and transcription units. Genome Res 2004;14:1902–10.
18. Ohm JE, McGarvey KM, Yu X, Cheng L, Schuebel KE, Cope L, et al. A stem cell-like chromatin pattern may predispose tumor suppressor genes to DNA hypermethylation and heritable silencing. Nat Genet 2007;39:237–42.
19. Widschwendter M, Fiegl H, Egle D, Mueller-Holzner E, Spizzo G, Marth C, et al. Epigenetic stem cell signature in cancer. Nat Genet 2007;39:157–8.
20. Emoto K, Yamada Y, Sawada H, Fujimoto H, Ueno M, Takayama T, et al. Annexin II overexpression correlates with stromal tenascin-C overexpression: a prognostic marker in colorectal carcinoma. Cancer 2001;92:1419–26.
21. Diaz VM, Hurtado M, Thomson TM, Reventos J, Paciucci R. Specific interaction of tissue-type plasminogen activator (t-PA) with Annexin II on the membrane of pancreatic cancer cells activates plasminogen and promotes invasion *in vitro*. Gut 2004;53:993–1000.

Published OnlineFirst July 6, 2011; DOI:10.1158/0008-5472.CAN-11-1076

22. Douma S, Van Laar T, Zevenhoven J, Meuwissen R, Van Garderen E, Peeper DS. Suppression of anoikis and induction of metastasis by the neurotrophic receptor TrkB. Nature 2004;430:1034–9.
23. Wang G, Wang Y, Shen C, Huang YW, Huang K, Huang TH, et al. RNA polymerase II binding patterns reveal genomic regions involved in microRNA gene regulation. PLoS One 2010;5:e13798.
24. Corcoran DL, Pandit KV, Gordon B, Bhattacharjee A, Kaminski N, Benos PV. Features of mammalian microRNA promoters emerge from polymerase II chromatin immunoprecipitation data. PLoS One 2009;4:e5279.
25. Fujita S, Iba H. Putative promoter regions of miRNA genes involved in evolutionarily conserved regulatory systems among vertebrates. Bioinformatics 2008;24:303–8.
26. Gu J, He T, Pei Y, Li F, Wang X, Zhang J, et al. Primary transcripts and expressions of mammal intergenic microRNAs detected by mapping ESTs to their flanking sequences. Mamm Genome 2006;17:1033–41.
27. Zhou X, Ruan J, Wang G, Zhang W. Characterization and identification of microRNA core promoters in four model species. PLoS Comput Biol 2007;3:e37.
28. Long YS, Deng GF, Sun XS, Yi YH, Su T, Zhao QH, et al. Identification of the transcriptional promoters in the proximal regions of human microRNA genes. Mol Biol Rep 2010.
29. Mikkelsen TS, Ku M, Jaffe DB, Issac B, Lieberman E, Giannoukos G, et al. Genome-wide maps of chromatin state in pluripotent and lineage-committed cells. Nature 2007;448:553–60.
30. Tsai KW, Kao HW, Chen HC, Chen SJ, Lin WC. Epigenetic control of the expression of a primate-specific microRNA cluster in human cancer cells. Epigenetics 2009;4:587–92.
31. Saito Y, Suzuki H, Tsugawa H, Nakagawa I, Matsuzaki J, Kanai Y, et al. Chromatin remodeling at Alu repeats by epigenetic treatment activates silenced microRNA-512-5p with downregulation of Mcl-1 in human gastric cancer cells. Oncogene 2009;28:2738–44.
32. Borchert GM, Lanier W, Davidson BL. RNA polymerase III transcribes human microRNAs. Nat Struct Mol Biol 2006;13:1097–101.
33. Jacinto FV, Ballestar E, Esteller M. Impaired recruitment of the histone methyltransferase DOT1L contributes to the incomplete reactivation of tumor suppressor genes upon DNA demethylation. Oncogene 2009;28:4212–24.
34. Ando T, Yoshida T, Enomoto S, Asada K, Tatematsu M, Ichinose M, et al. DNA methylation of microRNA genes in gastric mucosae of gastric cancer patients: its possible involvement in the formation of epigenetic field defect. Int J Cancer 2009;124:2367–74.
35. Agirre X, Vilas-Zornoza A, Jimenez-Velasco A, Martin-Subero JI, Cordeu L, Garate L, et al. Epigenetic silencing of the tumor suppressor microRNA Hsa-miR-124a regulates CDK6 expression and confers a poor prognosis in acute lymphoblastic leukemia. Cancer Res 2009;69:4443–53.
36. Huang YW, Liu JC, Deatherage DE, Luo J, Mutch DG, Goodfellow PJ, et al. Epigenetic repression of microRNA-129-2 leads to overexpression of SOX4 oncogene in endometrial cancer. Cancer Res 2009;69:9038–46.
37. Kozaki K, Imoto I, Mogi S, Omura K, Inazawa J. Exploration of tumor-suppressive microRNAs silenced by DNA hypermethylation in oral cancer. Cancer Res 2008;68:2094–105.
38. Balaguer F, Link A, Lozano JJ, Cuatrecasas M, Nagasaka T, Boland CR, et al. Epigenetic silencing of miR-137 is an early event in colorectal carcinogenesis. Cancer Res 2010;70:6609–18.
39. Sarver AL, French AJ, Borralho PM, Thayanithy V, Oberg AL, Silverstein KA, et al. Human colon cancer profiles show differential microRNA expression depending on mismatch repair status and are characteristic of undifferentiated proliferative states. BMC Cancer 2009;9:401.
40. Nasser MW, Datta J, Nuovo G, Kutay H, Motiwala T, Majumder S, et al. Down-regulation of micro-RNA-1 (miR-1) in lung cancer. Suppression of tumorigenic property of lung cancer cells and their sensitization to doxorubicin-induced apoptosis by miR-1. J Biol Chem 2008;283:33394–405.
41. Datta J, Kutay H, Nasser MW, Nuovo GJ, Wang B, Majumder S, et al. Methylation mediated silencing of MicroRNA-1 gene and its role in hepatocellular carcinogenesis. Cancer Res 2008;68:5049–58.
42. Hu Z, Chen X, Zhao Y, Tian T, Jin G, Shu Y, et al. Serum microRNA signatures identified in a genome-wide serum microRNA expression profiling predict survival of non-small-cell lung cancer. J Clin Oncol 2010;28:1721–6.
43. Yan D, Dong Xda E, Chen X, Wang L, Lu C, Wang J, et al. MicroRNA-1/206 targets c-Met and inhibits rhabdomyosarcoma development. J Biol Chem 2009;284:29596–604.
44. Croce CM. Causes and consequences of microRNA dysregulation in cancer. Nat Rev Genet 2009;10:704–14.
45. Maru DM, Singh RR, Hannah C, Albarracin CT, Li YX, Abraham R, et al. MicroRNA-196a is a potential marker of progression during Barrett's metaplasia-dysplasia-invasive adenocarcinoma sequence in esophagus. Am J Pathol 2009;174:1940–8.
46. Guan Y, Mizoguchi M, Yoshimoto K, Hata N, Shono T, Suzuki SO, et al. MiRNA-196 is upregulated in glioblastoma but not in anaplastic astrocytoma and has prognostic significance. Clin Cancer Res 2010;16:4289–97.
47. Liu X, Sempere LF, Galimberti F, Freemantle SJ, Black C, Dragnev KH, et al. Uncovering growth-suppressive MicroRNAs in lung cancer. Clin Cancer Res 2009;15:1177–83.
48. Lin SL, Chiang A, Chang D, Ying SY. Loss of mir-146a function in hormone-refractory prostate cancer. RNA 2008;14:417–24.
49. Bhaumik D, Scott GK, Schokrpur S, Patil CK, Campisi J, Benz CC. Expression of microRNA-146 suppresses NF-kappaB activity with reduction of metastatic potential in breast cancer cells. Oncogene 2008;27:5643–7.
50. Li Y, Vandenboom TG 2nd, Wang Z, Kong D, Ali S, Philip PA, et al. miR-146a suppresses invasion of pancreatic cancer cells. Cancer Res 2010;70:1486–95.

Co-expression of laminin β3 and γ2 chains and epigenetic inactivation of laminin α3 chain in gastric cancer

MASANORI II[1*], HIROYUKI YAMAMOTO[1*], HIROAKI TANIGUCHI[1], YASUSHI ADACHI[1], MAYUMI NAKAZAWA[1], HIROKAZU OHASHI[1], TOKUMA TANUMA[1], YASUTAKA SUKAWA[1], HIROMU SUZUKI[1], SHIGERU SASAKI[1], KOHZOH IMAI[2] and YASUHISA SHINOMURA[1]

[1]First Department of Internal Medicine, Sapporo Medical University, Sapporo, Hokkaido 060-8543; [2]The Institute of Medical Science, The University of Tokyo, Tokyo 108-8639, Japan

Received March 1, 2011; Accepted April 28, 2011

DOI: 10.3892/ijo.2011.1048

Abstract. Laminin-332 (LM-332, formerly termed laminin-5) is a heterotrimeric glycoprotein that regulates cell adhesion and migration. Molecular alterations of LM-332 are involved in cancer progression. The aim of this study was to clarify alterations of LM-332 in gastric carcinoma. The expression of LM-332 subunits in 10 gastric carcinoma cell lines was investigated by RT-PCR, Western blotting, and immunocytochemical/immunofluorescent analyses. The promoter methylation status of LM-332-encoding genes (LAMA3, LAMB3 and LAMC2) was analyzed by methylation-specific PCR (MSP). The relationship between cell migration and LM-332 expression was assessed by the scratch assay. The expression of LM-332 was analyzed immunohistochemically in 90 gastric cancer tissues. Co-expression of laminin β3 and γ2 chains was often observed in gastric carcinoma cell lines at mRNA and protein levels. In contrast, there was no expression of laminin α3 at either the mRNA or protein levels. Extracellular secretion of laminin β3 and γ2 chains was found in 2 of the 10 cell lines. The LAMA3 gene was transcriptionally silenced by methylation of the promoter CpG islands in all of the cell lines, while the LAMB3 and LAMC2 genes were silenced in several cell lines. Treatment with a demethylating agent, 5-aza-2'-deoxycytidine (5-aza-dC), restored expression of the LM-332-encoding genes. Methylation frequency of LAMA3 was higher than those of the LAMB2 and LAMC2 genes in gastric cancer tissues. Migration distances were significantly correlated with cytoplasmic laminin γ2 chain expression. Immunohistochemistry showed frequent co-expression of laminin β3 and γ2 chains in gastric carcinoma cells, which was significantly correlated with depth of invasion and advanced tumor stage. The results suggest that the laminin β3 and γ2 chains accumulate intracellularly and play a role in gastric cancer progression, while epigenetic silencing of the laminin α3 chain may lead to inability to synthesize the basement membrane and may affect cancer cell invasion. Cancer cell motility appears to be associated with the cytoplasmic laminin γ2 chain *in vitro*.

Introduction

The basement membrane (BM) is a supporting structure underlying the epithelium or endothelium. BM provides a scaffold for cellular growth and differentiation, and breakdown of the BM is now regarded as an essential step for tumor invasion and metastasis. Laminin, one of the major components of the BM, constitutes a family of at least 15 distinct isoforms in humans (1,2). The laminin molecule is a cross-shaped heterotrimer assembled from α, β and γ glycoprotein subunits. Five α, three β, and three γ subunits are known at present. Each member of the laminin family is currently designated on the basis of a system in which their trimers can be identified by Arabic numerals for three α, β, and γ chain numbers.

Laminin-332 (LM-332, formerly termed laminin-5) is a heterotrimer of α3, β3 and γ2 subunits, which are encoded by three distinct genes (LAMA3, LAMB3 and LAMC2, respectively). LM-332 interacts with integrin α6β4 in a hemidesmosome and supports various cellular functions, i.e., adhesion to the BM, proliferation, migration, polarity, and apoptosis (2,3). Three subunits of LM-332 are synthesized separately, and subsequent formation of a heterotrimer is an essential step for the final composition of LM-332.

Neoplastic transformation essentially involves alterations of cell-cell and cell-matrix adhesion molecules between the epithelium and BM. The amount and distribution of LM-332 also undergo diverse changes during carcinogenesis. In colorectal carcinogenesis, the distribution of LM-332 is preserved

Correspondence to: Dr Hiroyuki Yamamoto, First Department of Internal Medicine, Sapporo Medical University, South-1, West-16, Chuo-ku, Sapporo 060-8543, Japan
E-mail: h-yama@sapmed.ac.jp

*Contributed equally

Abbreviations: 5-aza-dC, 5-aza-2'-deoxycytidine; BM, basement membrane; LM-332, laminin-332; MSP, methylation-specific PCR; RT-PCR, reverse transcription-polymerase chain reaction; TSA, trichostatin A

Key words: laminin-332, gastric cancer, methylation, laminin γ2, cell motility

in the BM of adenomas but becomes discontinuous or reduced in carcinomas (4), resulting in loss of the BM. Several lines of evidence have demonstrated that the laminin γ2 monomer is overexpressed in invasive colorectal carcinoma, and this has been attributed to synergistic activation of the LAMC2 gene by TGF-β1 and HGF (5). We have reported that the laminin γ2 monomer is overexpressed in esophageal squamous cell carcinoma cells at the invasive front (6). Extracellular deposition or cytoplasmic accumulation of the laminin γ2 monomer has been reported in gastric adenocarcinoma (7,8). However, little is known about distribution patterns of LM-332 subunits in gastric carcinoma.

In this study, we investigated the expression patterns of both the mRNA and protein of LM-332 subunits and the relationship of migration activity with LM-322 expression in gastric cancer cell lines. Epigenetic alterations of the LAMA3, LAMB3, and LAMC2 genes were also analyzed. Finally, expression of LM-332 subunits was analyzed immunohistochemically in gastric cancer tissues.

Materials and methods

Cell culture and reagents. Ten human gastric cancer cell lines, NUGC3, SNU1, SNU638, AZ521, JRST, KATOIII, MKN7, MKN28, MKN45, and MKN74, were obtained from the Japanese Cancer Research Resources Bank (Tokyo, Japan), Riken Cell Bank (Tokyo), or the American Type Culture Collection (Rockville, MD, USA). The cells were grown in RPMI-1640 medium (GIBCO BRL) containing 10% fetal bovine serum at 37°C in a humidified atmosphere of 5% CO_2 in air.

Semiquantitative reverse transcription-polymerase chain reactions (RT-PCR). Expression of LAMA3, LAMB3, and LAMC2 was analyzed by semiquantitative RT-PCR. Total RNA was extracted from the cell lines. cDNA was synthesized from total RNA. Aliquots of cDNA (400 ng/μl) were subjected to PCR. cDNA generated from a human hepatoma cell line HuH-7 was used as a positive control for the LAMA3 gene, which was tested in our preliminary experiment (data not shown). GAPDH gene served as an internal control. Negative control reactions were run without a template cDNA. The sequences of PCR primers and thermal cycling conditions for amplifying each gene was determined as described previously (9,10). PCR products were electrophoresed on 2% agarose gels and visualized by ethidium bromide under UV illumination. All PCR reactions were done at least twice to validate the results.

Preparation of cell lysates. Protein extracts of cells were prepared by scraping lysed cells in RIPA lysis buffer (1% Nonidet P-40, 0.5% sodium deoxycholate (w/v), 0.1% SDS (w/v), and protease inhibitors in TBS). Samples were diluted and adjusted to the same protein concentration for quantitative Western blot analyses.

Preparation of conditioned media. To prepare conditioned media, cells were grown to semiconfluence in RPMI-1640 medium containing 10% FBS. The semiconfluent cultures were washed twice with PBS and incubated in serum-free RPMI-1640 medium for two days. MKN7 cells were incubated for about five days because this cell grew far slower than did other cell lines. The serum-free culture supernatants were collected and centrifuged at low speed to remove floating cells and debris. Proteins were concentrated 100-fold by a ultrafiltration method using a concentrator (Millipore). Samples were subjected to subsequent Western blot analysis.

Antibodies. Antibodies used for Western blot analysis, immunocytochemistry, and immunohistochemistry were rabbit polyclonal anti-laminin α3, goat polyclonal anti-laminin α3, rabbit polyclonal anti-laminin β3 (Santa Cruz Biotechnology), mouse monoclonal anti-laminin γ2 (Chemicon), and mouse monoclonal anti-actin (Thermo Fisher Scientific). All antibodies were applied at the concentration suggested by the manufacturer.

Western blot analyses for cell lysates and conditioned media. Samples of cell lysates and conditioned media were analyzed by conventional Western blot method. Proteins were resolved on 4-12% Bis-Tris gels (Invitrogen) under reducing condition. No protein controls were also electrophoresed, subsequently transferred to a PVDF membrane. Visualization was performed by chemiluminescence with specific antibodies.

Immunocytochemistry and immunofluorescence. Ten gastric cancer cell lines were cultured in Lab-Tek II CC2 Chamber Slide System (Thermo Fisher Scientific) in RPMI-1640 medium supplemented with 10% FBS. The media were removed and slides were washed with PBS. Cells were fixed in 4% paraformaldehyde for 15 min and permeabilized with 0.3% Triton X-100 with PBS. After blocking with 3% FBS in PBS, endogenous peroxidase was quenched by 3% hydrogen peroxidase for 10 min. Slides were wiped again and incubated with a primary antibody against laminin β3 or laminin γ2 chain. Rabbit or mouse normal immunoglobulins were substituted for each primary antibody as negative controls. Detection of the laminin β3 chain was carried out by a biotinylated IgG and peroxidase-conjugated streptavidin kit (DakoCytomation), followed by development with 0.04% (w/v) diaminobenzidine solution with 0.01% hydrogen peroxidase for 5 min. Hematoxylin was used for counterstain. For an immunofluorescence study for the laminin γ2 chain, secondary antibody was conjugated to Alexa fluor 555 (Molecular Probes), and 4', 6-diamidino-2-phenylindole (DAPI) was used for nuclear counterstain. Slides were mounted with aqueous mounting medium and sealed with coverslip. All staining procedures were carried out with a standard method to minimize variability.

Methylation-specific PCR (MSP). Methylation status of CpGs in the promoter regions of the LAMA3, LAMB3, and LAMC2 genes were determined by conventional MSP. Genomic DNA was extracted from the cell lines and 50 gastric cancer tissues. Informed consent was obtained from each patient. DNA was treated with sodium bisulfite using EZ DNA Methylation-Gold kit (ZYMO Research) and subjected to MSP. To detect methylation status of CpGs in the promoter regions of the LAMA3, LAMB3, and LAMC2 genes, two pairs of MSP primers specific for methylated or unmethylated alleles were used at appropriate temperature as described previously (11).

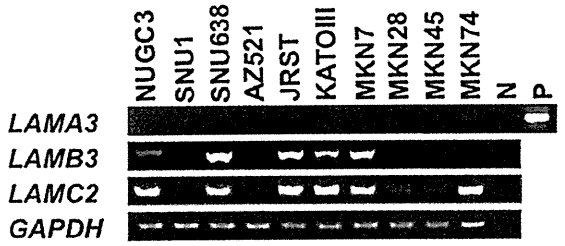

Figure 1. Expression of mRNA of the LM-332 encoding genes in gastric cancer cell lines analyzed by RT-PCR. HuH-7 cDNA served as a positive control for the LAMA3 gene. GAPDH was used as an internal control.

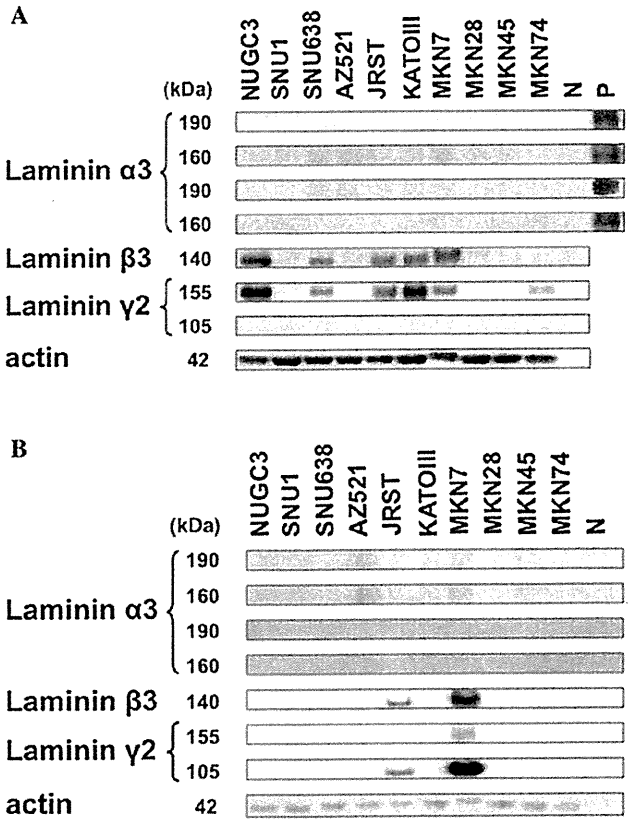

Figure 2. Protein expression of LM-332 in gastric cancer cell lines. (A) Western blot analyses for cell lysates. (B) Western blot analyses for conditioned media.

No template controls were used in the assays. MSP products were visualized on 2% TBE agarose gels containing 0.25 μg/ml ethidium bromide. Each sample was tested at least in duplicate.

5-aza-2'-deoxycytidine (5-aza-dC) and/or trichostatin A (TSA) treatment. To examine the role of CpG methylation and histone deacetylation in silencing of laminin-332-encoding genes, cancer cells were treated with 2 or 5 μM of 5-aza-dC (Sigma, St. Louis, MO, USA) for 72 h or with 100 nM of TSA for 24 h. Cells were also treated with 2 or 5 μM of 5-aza-dC for 72 h followed by 600 nM of TSA for an additional 24 h. The timing and sequencing of 5-aza-dC and/or TSA was based on similar preliminary studies as well as published studies (11,12). After the treatment, expression of laminin-332-encoding genes was analyzed by RT-PCR.

In vitro migration assay (scratch assay). Cells ($1x10^6$/well) of eight cell lines (except MKN7 and KATOIII) were seeded onto 6-well plates and cultured in RPMI-1640 medium with 10% FBS overnight at 37°C with 5% CO_2. When the cells were semiconfluent, a straight scratch was gently made through the central axis of the plate using a pipette tip. The plates were rinsed with PBS and culture media were replaced. Initial widths of the scratches were immediately measured. After 24 h of incubation, the distance that remaining cells migrated across the scratch line was measured as described previously (13). Quantification was performed by photoshop. All scratch assays were done in triplicate. The results were expressed as the means ± SD.

Immunohistochemistry of gastric cancer tissues. Tissue microarray of gastric cancer tissues was purchased from SuperBioChips Laboratories (Seoul, Korea) and used for immunohistochemical analysis. Immunohistochemistry was carried out as described previously (3). Normal rabbit or mouse immunoglobulins were used as negative controls. Cytoplasmic expression was defined as positive when immunoreactivity was observed in >10% of carcinoma cells.

Statistical analysis. Statistical significance of associations between the migration distances and the relative quantitative levels of laminin γ2 protein in Western blot was determined by Pearson's correlation test. The correlation between immunohistochemical expression and clinicopathological characteristics was determined by the following statistical tests: Student's t-test for age, the Mann-Whitney test for lymph node metastasis and pTNM stage, and the χ^2 test or Fisher's exact test for the remaining parameter. A P-value of ≤0.05 was considered significant.

Results

Coexpression of LAMB3 and LAMC2 mRNA in gastric cancer cell lines. Results of RT-PCR analyses are shown in Fig. 1. LAMB3 was intensely detected in 40% of the cell lines (SNU638, JRST, KATOIII and MKN7) and weakly detected in NUGC3 cells. LAMC2 was intensely detected in 60% of the cell lines (NUGC3, SNU638, JRST, KATOIII, MKN7 and MKN74) and very weakly detected in MKN28 and MKN45 cells. Notably, LAMA3 was not amplified after 35 PCR cycles in any of the tested cell lines, even in triplicate experiments. Expression of three LM-332-encoding genes was not associated with histological type (intestinal/diffuse type) or histological grade (poor/moderately/well-differentiated adenocarcinoma) of gastric cancer cell lines.

Intracellular coexpression of laminin β3 and γ2 proteins in gastric cancer cell lines. Cell lysate proteins were subjected to Western blot analyses for evaluation of intracellular synthesis of laminin-332 subunits (Fig. 2A). Laminin β3 protein was detected in 50% of cell lines (NUGC3, SNU638, JRST, KATOIII, and MKN7). Nonprocessed laminin γ2 protein

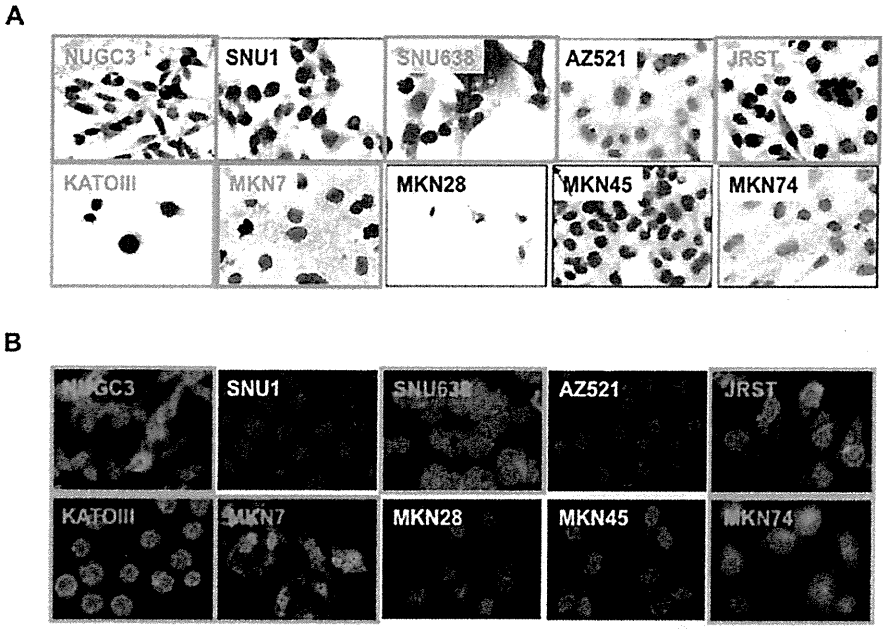

Figure 3. Immunocytochemistry for the laminin β3 chain and double immunofluorescent staining for the laminin γ2 chain in gastric cancer cell lines. (A) Immunocytochemistry for the laminin β3 chain. Positive staining is brown and nuclei counterstain is hematoxylin. Original magnification, x400. (B) Double immunofluorescent staining for the laminin γ2 chain. Nuclei were counterstained with DAPI (blue). Original magnification, x400.

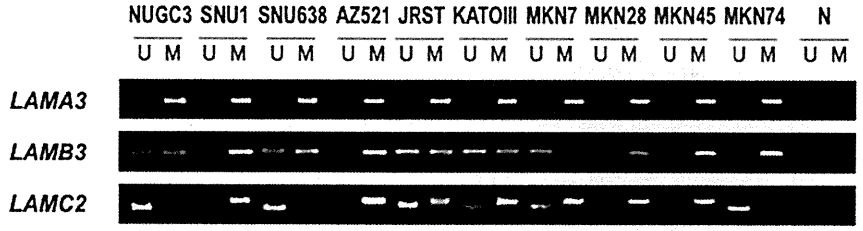

Figure 4. MSP analyses for the LM-332-encoding genes in gastric cancer cell lines. U, unmethylated PCR products; M, methylated PCR products.

(155 kDa) was detected in 60% of cell lines (NUGC3, SNU638, JRST, KATOIII, MKN7, and MKN74). Processed laminin γ2 protein (105 kDa) was not detected in any of the cell lines. Remarkably, laminin β3 and γ2 proteins were coexpressed in 50% of cell lines (NUGC3, SNU638, JRST, KATOIII and MKN7). The presence of laminin β3 and γ2 proteins was consistent with the presence of the LAMB3 and LAMC2 mRNA. Neither the non-processed (190 kDa) nor processed (160 kDa) form of laminin α3 protein was found in any of the cell lines despite the use of two kinds of antibodies.

Expression of laminin β3 and γ2 proteins released by gastric cancer cell lines. In Western blot analysis for conditioned media, neither non-processed (190 kDa) nor processed (160 kDa) laminin α3 proteins were found in any of the cell lines despite the use of two kinds of antibodies (Fig. 2B). The laminin β3 chain was detected in JRST and MKN7 cells. The non-processed laminin γ2 chain (155 kDa) was identified only in MKN7 cells. Noteworthy, the processed laminin γ2 chain (105 kDa) was also detected in JRST and MKN7 cells. The latter was not observed in Western blot analysis of the cell lysates. The other eight cell lines did not release any LM-332 subunits into the conditioned media.

Visualization of laminin β3 and γ2 proteins by immunocytochemical examination. Cultured cells on the chamber slides were subjected to immunocytochemical examination for evaluation of the expression of laminin β3 and γ2 chains (Fig. 3). There was no detectable immunoreactivity with a control antibody (data not shown). The laminin β3 chain was specifically immunostained in the cytoplasm of 50% of the cell lines (NUGC3, SNU638, JRST, KATOIII and MKN7). By means of intuitively comparing the saturation of fluorescent dye, the laminin γ2 chain was found in the cytoplasm of 60% of the cell lines (NUGC3, SNU638, JRST, KATOIII, MKN7, and MKN74). The results of both stainings were consistent with those of RT-PCR and Western blot analyses for cell lysates.

Methylation of the LAMA3 promoter correlates with lack of LAMA3 expression. MSP analysis showed PCR products for unmethylated and methylated promoter regions of the LAMA3, LAMB3 and LAMC2 genes (Fig. 4). Notably, the LAMA3 promoter was methylated in all of the 10 cell lines. The LAMB3 promoter was methylated in 50% of the cell lines (SNU1, AZ521, MKN28, MKN45 and MKN74) and partially unmethylated in the remaining cell lines. The

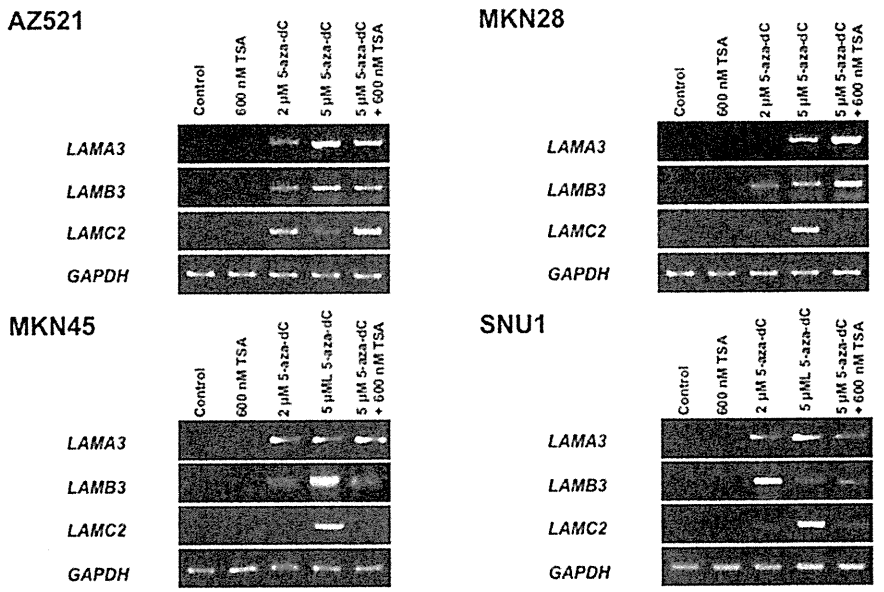

Figure 5. Re-activation of the LM-332 encoding genes by 5-aza-dC treatment in gastric cancer cell lines. As indicated, cells were incubated for 72 h with 2 μM or 5 μM 5-aza-dC and/or for 24 h with 600 nM TSA. After the treatment, expression of the LM-332 encoding genes was analyzed by RT-PCR.

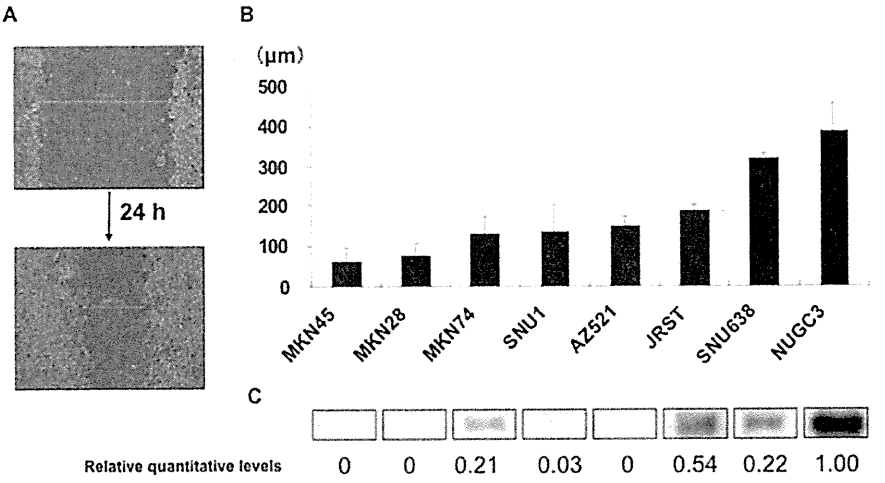

Figure 6. A correlation between migration analyzed by scratch assay and laminin γ2 expression. (A) Representative images of straight scratch made in the migration assay. Bar, 612.9 and 286 μm. (B) Distance that cells migrated across the scratch line. C, Cytoplasmic laminin γ2 expression analyzed by Western blotting is also shown side by side. Relative quantitative levels are shown below band images. The migration distances were significantly correlated with the quantitative levels of laminin γ2 proteins ($p<0.05$).

LAMC2 promoter was methylated in 40% of the cell lines (SNU1, AZ521, MKN28, and MKN45) and partially or completely unmethylated in the remaining cell lines. The methylation status of LAMB3 and LAMC promoters was consistent with the lack of gene expression determined by RT-PCR.

Re-activation of the laminin-332-encoding genes expression by 5-aza-dC/TSA treatment. To further examine the role of CpG methylation and histone deacetylation in silencing of the laminin-332-encoding genes, cancer cell lines were treated with 5-aza-dC and/or TSA. 5-aza-dC restored expression of the laminin-332-encoding genes in cancer cell lines (Fig. 5). Treatment with TSA alone had no effect. Combined treatment with 5-aza-dC and TSA restored expression of the laminin-332-encoding genes synergistically in several cancer cell lines.

Migration activity is associated with laminin γ2 protein expression. In the scratch assay, NUGC3, SNU638 and JRST were more motile than other cell lines (Fig. 6A and B). The migration distances were significantly correlated with quantitative levels of cytoplasmic laminin γ2 proteins determined by Western blot analysis ($p<0.05$; Fig. 6C).

Methylation of laminin-332-encoding genes in gastric cancer tissues. Methylation status of laminin-332-encoding genes was analyzed by MSP in gastric cancer tissues. Methylation of

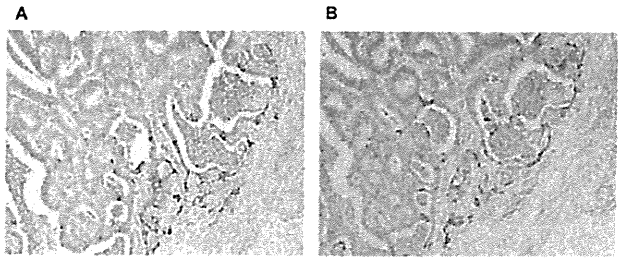

Figure 7. Representative results of immunohistochemistry for laminin β3 (A) and γ2 (B) in gastric cancer tissues. Original magnification, x400.

LAMA3, LAMB2 and LAMC2 genes was detected in 70, 24 and 20% of the 50 gastric cancer tissues, respectively. Methylation frequency of LAMA3 was significantly higher than methylation frequencies of LAMB2 and LAMC2 in gastric cancer tissues ($p<0.001$). Methylation status of laminin-332-encoding genes was not siginificantly correlated with clinicopathological features (data not shown).

Association of the expression of laminin β3 and γ2 chains with clinicopathological characteristics. Fig. 7 shows representative results of immunohistochemistry for laminin β3 and γ2 chains. Expression of laminin α3 was detected in normal BMs but not in carcinoma cells (data not shown). There was no detectable immunoreactivity with negative controls (data not shown). Positive staining for laminin β3 and γ2 chains in the cytoplasm of carcinoma cells was observed in 50 (56%) and 53 (59%) of the gastric cancer tissues. Notably, laminin β3 and γ2 chains were significantly coexpressed ($p< 0.05$). For both laminin β3 and γ2 chains, positivity was significantly correlated with depth of invasion and advanced tumor stage ($p<0.05$).

Discussion

In the present study, analysis of expression profiles of laminin-332-encoding genes by RT-PCR showed that LAMB3 mRNA and LAMC2 mRNA were often coexpressed in gastric cancer cell lines. These results suggest that LAMB3 and LAMC2 genes are regulated by a similar mechanism or undergo gene transcription dependently. In contrast, LAMA3 mRNA expression was not detected in any of the cell lines, suggesting that transcription of the LAMA3 gene is regulated by a mechanism different from that for LAMB3 and LAMC2 genes.

Coexpression of laminin β3 and γ2 chains in gastric cancer cell lines was further supported by results of Western blot analyses of cultured cell lysates and immunostaining. These results suggest that cultured gastric cancer cells generate laminin β3 and γ2 chains during autonomous growth *in vitro*.

Of note, laminin β3 and γ2 chains were also assumed to be secreted into culture media by JRST and MKN7 cell lines. This notion is supported by previous data showing that tumor cell lines expressing laminin β3 and γ2 chains, but not the α3 chain, could secrete γ2 monomer or β3γ2 heterodimer (14,15). Simultaneous detection of processed (105 kDa) and nonprocessed (155 kDa) laminin γ2 chain in the conditioned medium of MKN7, which was not observed in the cell lysate of MKN7, is consistent with the results of a previous study showing that a γ2 subunit is digested into a mature form after extracellular secretion (16).

By using MSP, we demonstrated that silencing of the LM-332-encoding genes was correlated with hypermethylation of the promoter in gastric cancer cell lines. To confirm the role of epigenetic alterations in transcriptional repression of the LM-332-encoding genes, we treated gastric cancer cell lines, in which the LM-332-encoding genes was methylated, with 5-aza-dC alone or in combination with TSA. Treatment with 5-aza-dC restored the LM-332-encoding genes expression in cancer cell lines. Moreover, combined treatment with 5-aza-dC and TSA restored expression synergistically, indicating CpG methylation and histone deacetylation have an important role in silencing the LM-332-encoding genes.

Epigenetic inactivation of LM-332-encoding genes through aberrant promoter methylation has been reported in lung, bladder, breast, and prostate cancer cell lines and cancer tissues (11,17-19). Frequencies of LAMA3 methylation have generally been higher than frequencies of methylation of LAMB3 and LAMC. Similar results were obtained in the present study, suggesting that epigenetic regulation of LM-332-encoding genes, especially LAMA3 silencing, plays a role in the progression of gastric cancer. The LM-332 molecule has been demonstrated to be synthesized initially as three monomers of each subunit, which are then glycosylated (16). Subsequently, β3 and γ2 chains assemble into a β3γ2 heterodimer, followed by incorporation of the α3 subunit to form an α3β3γ2 heterotrimer. Therefore, frequent laminin α3 chain suppression due to DNA methylation may play a critical role in the cytoplasmic accumulation of laminin β3 and γ2 chains in gastric cancer cells.

The laminin γ2 monomer is frequently expressed in invasive carcinomas and has recently been recognized as an excellent invasion marker for epithelial tumors (3,6-8). In this regard, it is interesting that cytoplasmic laminin γ2 chain expression was significantly associated with gastric cancer cell motility *in vitro* as shown by the migration assay. LM-332 is a constituent of the BM that provides static adhesion and hemidesmosome formation, but the monomeric laminin γ2 chain does not act as a morphogenesis protein. The results suggest that the cytoplasmic laminin γ2 chain plays a positive role in gastric cancer cell motility.

The results of *in vitro* expression studies were further supported by results for primary tumor tissues. Laminin β3 and γ2 chains were often coexpressed in cancer cells of gastric cancer tissues, and both of them were associated with depth of invasion and advanced tumor stage. The results suggest that coexpression of laminin β3 and γ2 chains is involved in the aggressive phenotype of gastric cancer cells, resulting in the progression of disease. Previous immunohistochemical studies have shown significant coexpression of laminin β3 and γ2 chains in the cytoplasm of invading or budding tumor cells in colorectal carcinoma, lingual squamous cell carcinoma, hepatocellular carcinoma, and basal cell carcinoma of the skin (4,9,20,21). We have also reported overexpression of laminin β3 and γ2 chains in biliary cancer (3). Our results further support the notion that laminin β3 and γ2 chains play an important role in cancer progression.

Mechanisms underlying cytoplasmic accumulation of laminin β3 and γ2 chains in cancer cells *in vivo* are not

known. Firstly, interactions of cancer cells with stromal cells may promote an accumulation of laminin β3 and γ2 chains (3). Secondly, it is thought that suppression of α3 chain expression may hinder LM-332 trimer secretion, leading to abnormal accumulation of the β3γ2 heterodimer (4). Our results support the latter possibility, but further investigation is necessary.

Loss of any of the five component chains of the laminin-integrin complex (LM-332 and α6β4) could disrupt the hemidesmosome and BM, leading to cancer cell invasion (11,18). Loss of LM-332 could favor disassembly or reduction in the number of hemidesmosomes with a consequent failure of cell anchoring, leading to an invasive and metastatic phenotype (11). While loss of any chains results in loss of the functional molecule, expression of one or more chains (especially β3 and γ2) may promote cancer cell invasion (2). Since LM-332 is a component of the BM, which is a major barrier for invasion of cancer, detection of methylation of LM-332-encoding genes may be useful for distinguishing aggressive gastric cancers from non-aggressive ones (11).

Acknowledgements

This study was supported by Grants-in-Aid for Scientific Research from the Ministry of Education, Culture, Sports, Science and Technology of Japan (H.Y., K.I. and Y.S.) and supported in part by Program for developing the supporting system for upgrading the education and research from the Ministry of Education, Culture, Sports, Science, and Technology (Y.S.).

References

1. Colognato H and Yurchenco PD: Form and function: the laminin family of heterotrimers. Dev Dyn 218: 213-234, 2000.
2. Giannelli G and Antonaci S: Biological and clinical relevance of laminin-5 in cancer. Clin Exp Metastasis 18: 439-443, 2000.
3. Oka T, Yamamoto H, Sasaki S, Ii M, Hizaki K, Taniguchi H, Adachi Y, Imai K and Shinomura Y: Overexpression of β3/γ2 chains of laminin-5 and MMP7 in biliary cancer. World J Gastroenterol 15: 3865-3873, 2009.
4. Sordat I, Bosman FT, Dorta G, Rousselle P, Aberdam D, Blum AL and Sordat B: Differential expression of laminin-5 subunits and integrin receptors in human colorectal neoplasia. J Pathol 185: 44-52, 1998.
5. Olsen J, Kirkeby LT, Brorsson MM, Dabelsteen S, Troelsen JT, Bordoy R, Fenger K, Larsson L-I and Simon-Assmann P: Converging signals synergistically activate the LAMC2 promoter and lead to accumulation of the laminin gamma 2 chain in human colon carcinoma cells. Biochem J 371: 211-221, 2003.
6. Yamamoto H, Itoh F, Iku S, Hosokawa M and Imai K: Expression of the γ2 chain of laminin-5 at the invasive front is associated with recurrence and poor prognosis in human esophageal squamous cell carcinoma. Clin Cancer Res 7: 896-900, 2001.
7. Koshikawa N, Moriyama K, Takamura H, Mizushima H, Nagashima Y, Yanoma S and Miyazaki K: Overexpression of laminin γ2 chain monomer in invading gastric carcinoma cells. Cancer Res 59: 5596-5601, 1999.
8. Yamamoto H, Kitadai Y, Yamamoto H, Oue N, Ohdan H, Yasui W and Kikuchi A: Laminin gamma2 mediates Wnt5a-induced invasion of gastric cancer cells. Gastroenterology 137: 242-252, 2009.
9. Giannelli G, Fransvea E, Bergamini C, Marinosci F and Antonaci S: Laminin-5 chains are expressed differentially in metastatic and nonmetastatic hepatocellular carcinoma. Clin Cancer Res 9: 3684-3691, 2003.
10. Giannelli G, Bergamini C, Fransvea E, Sgarra C and Antonaci S: Laminin-5 with transforming growth factor-beta 1 induces epithelial to mesenchymal transition in hepatocellular carcinoma. Gastroenterology 129: 1375-1383, 2005.
11. Sathyanarayana UG, Toyooka S, Padar A, Takahashi T, Brambilla E, Minna JD and Gazdar AF: Epigenetic inactivation of laminin-5-encoding genes in lung cancers. Clin Cancer Res 9: 2665-2672, 2003.
12. Cameron EE, Bachman KE, Myohanen S, Myöhänen S, Herman JG and Baylin SB: Synergy of demethylation and histone deacetylase inhibition in the re-expression of genes silenced in cancer. Nat Genet 21: 103-107, 1999.
13. Zhou Y, Zhang J, Liu Q, Bell R, Muruve DA, Forsyth P, Arcellana-Panlilio M, Robbins S and Yong VW: The chemokine GRO-α (CXCL1) confers increased tumorigenicity to glioma cells. Carcinogenesis 26: 2058-2068, 2005.
14. Niessen CM, Hogervorst F, Jaspars LH, de Melker AA, Delwel GO, Hulsman EH, Kuikman I and Sonnenberg A: The alpha 6 beta 4 integrin is a receptor for both laminin and kalinin. Exp Cell Res 211: 360-367, 1994.
15. Mizushima H, Miyagi Y, Kikkawa Y, Yamanaka N, Yasumitsu H, Misugi K and Miyazaki K: Differential expression of laminin-5/ladsin subunits in human tissues and cancer cell lines and their induction by tumor promoter and growth factors. J Biochem 120: 1196-1202, 1996.
16. Matsui C, Wang CK, Nelson CF, Bauer EA and Hoeffler WK: The assembly of laminin-5 subunits. J Biol Chem 270: 23496-23503, 1995.
17. Sathyanarayana UG, Maruyama R, Padar A, Suzuki M, Bondaruk J, Sagalowsky A, Minna JD, Frenkel EP, Grossman HB, Czerniak B and Gazdar AF: Molecular detection of noninvasive and invasive bladder tumor tissues and exfoliated cells by aberrant promoter methylation of laminin-5 encoding genes. Cancer Res 64: 1425-1430, 2004.
18. Sathyanarayana UG, Padar A, Huang CX, Suzuki M, Shigematsu H, Bekele BN and Gazdar AF: Aberrant promoter methylation and silencing of laminin-5-encoding genes in breast carcinoma. Clin Cancer Res 9: 6389-6394, 2003.
19. Sathyanarayana UG, Padar A, Suzuki M, Maruyama R, Shigematsu H, Hsieh J-T, Frenkel EP and Gazdar AF: Aberrant promoter methylation of laminin-5-encoding genes in prostate cancers and its relationship to clinicopathological features. Clin Cancer Res 9: 6395-6400, 2003.
20. Akimoto S, Nakanishi Y, Sakamoto M, Kanai Y and Hirohashi S: Laminin 5 beta3 and gamma2 chains are frequently coexpressed in cancer cells. Pathol Int 54: 688-692, 2004.
21. Svensson Mansson S, Reis-Filho J and Landberg G: Transcriptional upregulation and unmethylation of the promoter region of p16 in invasive basal cell carcinoma cells and partial co-localization with the gamma 2 chain of laminin-332. J Pathol 212: 102-111, 2007.

Published OnlineFirst June 3, 2011; DOI:10.1158/1078-0432.CCR-10-3131

Cancer Therapy: Preclinical

Clinical Cancer Research

The Efficacy of IGF-I Receptor Monoclonal Antibody against Human Gastrointestinal Carcinomas is Independent of *k-ras* Mutation Status

Masanori Ii[1], Hua Li[1], Yasushi Adachi[1], Hiroyuki Yamamoto[1], Hirokazu Ohashi[1], Hiroaki Taniguchi[1], Yoshiaki Arimura[1], David P. Carbone[2,3], Kohzoh Imai[4], and Yasuhisa Shinomura[1]

Abstract

Purpose: Insulin-like growth factor (IGF)-I receptor (IGF-IR) signaling is required for carcinogenicity and proliferation of gastrointestinal cancers. We have previously shown successful targeting therapy for colorectal, pancreatic, gastric, and esophageal carcinomas using recombinant adenoviruses expressing dominant negative IGF-IR. Mutation in *k-ras* is one of key factors in gastrointestinal cancers. In this study, we sought to evaluate the effect of a new monoclonal antibody for IGF-IR, figitumumab (CP-751,871), on the progression of human gastrointestinal carcinomas with/without *k-ras* mutation.

Experimental Design: We assessed the effect of figitumumab on signal transduction, proliferation, and survival in six gastrointestinal cancer cell lines with/without *k-ras* mutation, including colorectal and pancreatic adenocarcinoma, esophageal squamous cell carcinoma, and hepatoma. Combination effects of figitumumab and chemotherapy were also studied. Then figitumumab was evaluated in the treatment of xenografts in nude mice.

Results: Figitumumab blocked autophosphorylation of IGF-IR and its downstream signals. The antibody suppressed proliferation and tumorigenicity in all cell lines. Figitumumab inhibited survival by itself and up-regulated chemotherapy (5-FU and gemcitabine) induced apoptosis. Moreover, the combination of this agent and chemotherapy was effective against tumors in mice. The effect of figitumumab was not influenced by the mutation status of *k-ras*. Figitumumab reduced expression of IGF-IR but not insulin receptor in these xenografted tumors. The drug did not affect murine body weight or blood concentrations of glucose, insulin, IGF binding protein 3, and growth hormone.

Conclusions: IGF-IR might be a good molecular therapeutic target and figitumumab may thus have therapeutic value in human gastrointestinal malignancies even in the presence of *k-ras* mutations. *Clin Cancer Res; 17(15); 5048–59. ©2011 AACR.*

Introduction

Gastrointestinal (GI) cancers encompass a variety of diseases, many of whose prognoses are poor. Although only colorectal cancer is listed in the top 10 for incidence rates of cancer in the USA, 4 GI cancers, including colorectal, pancreas, liver and the biliary tract, and esophageal, are in the top 10 for death rates from cancer (1). In Japan, there are 5 GI cancers, including colorectal, gastric, pancreatic, hepatic, and biliary tract, in the top 10 for death rates in 2007. Therefore, we must to seek new therapeutic options for GI cancers.

Signals from a variety of growth factors are required for tumorigenesis and cancer development in human malignancies (2, 3). Recently, advances in molecular cancer research have brought new therapeutic forces from the bench into clinic. One group of new targets is the receptor tyrosine kinases for which specific small molecule tyrosine kinase inhibitors (TKIs) or blocking monoclonal antibodies (mAbs) exist. Type I insulin-like growth factor (IGF)-I receptor (IGF-IR) could be the next important molecular target (3, 4).

Binding of the ligands, IGF-I and IGF-II, to IGF-IR causes receptor autophosphorylation and activates multiple signaling pathways, including the mitogen-activated protein kinase (MAPK, extracellular signal-regulated kinase [ERK]) and phosphatidylinositide 3-kinase (PI3-K)/Akt-1 pathways (5–7). These can stimulate tumor progression and cellular differentiation (8). IGF-IR axis function is also regulated by IGF binding proteins (IGFBPs) and type 2 IGF receptor (IGF-IIR; refs. 9–11).

Authors' Affiliations: [1]First Department of Internal Medicine, Sapporo Medical University, Sapporo, Japan; Departments of [2]Medicine and [3]Cell Biology, Vanderbilt-Ingram Cancer Center and Vanderbilt University, Nashville, Tennessee; and [4]The Institute of Medical Science, The University of Tokyo, Tokyo, Japan

Note: M. Ii, H. Li, and Y. Adachi contributed equally to this work.

Corresponding Author: Yasushi Adachi, First Department of Internal Medicine, Sapporo Medical University, S-1, W-16, Chuo-ku, Sapporo 060-8543, Japan. Phone: +81-11-611-2111(ext. 3211); Fax: +81-11-611-2282; E-mail: yadachi@sapmed.ac.jp

doi: 10.1158/1078-0432.CCR-10-3131